DEVCOM DAC-TR-2022-033
April 2022

Pelvis–Lumbar Spine Injury Trade-off Investigation Studies at the Medical College of Wisconsin

by Narayan Yoganandan, Jason Moore, John R. Humm, Frank A. Pintar,
Jamie Baisden, David R. Barnes, and Kathryn L. Loftis

DISCLAIMER

The findings in this report are not to be construed as an official Department of the Army position unless so specified by other official documentation.

WARNING

Information and data contained in this document are based on the input available at the time of preparation.

TRADE NAMES

The use of trade names in this report does not constitute an official endorsement or approval of the use of such commercial hardware or software. The report may not be cited for purposes of advertisement.

DEVCOM DAC-TR-2022-033
April 2022

Pelvis–Lumbar Spine Injury Trade-off Investigation Studies at the Medical College of Wisconsin

by Narayan Yoganandan, Jason Moore, John R. Humm, Frank A. Pintar, and Jamie Baisden
Medical College of Wisconsin

David R. Barnes
SURVICE Engineering Company

Kathryn L. Loftis
DEVCOM Analysis Center

REPORT DOCUMENTATION PAGE

Form Approved
OMB No. 0704-0188

1. REPORT DATE	2. REPORT TYPE	3. DATES COVERED (From - To)
April 2022	Technical Report	October 2021–March 2022

4. TITLE AND SUBTITLE
Pelvis–Lumbar Spine Injury Trade-off Investigation Studies at the Medical College of Wisconsin

5a. CONTRACT NUMBER

5b. GRANT NUMBER

5c. PROGRAM ELEMENT NUMBER

6. AUTHOR(S)
Narayan Yoganandan, Jason Moore, John R. Humm, Frank A. Pintar, Jamie Baisden, David R. Barnes, and Kathryn L. Loftis

5d. PROJECT NUMBER

5e. TASK NUMBER

5f. WORK UNIT NUMBER

7. PERFORMING ORGANIZATION NAME(S) AND ADDRESS(ES)
Director
DEVCOM Analysis Center
6896 Mauchly Street
Aberdeen Proving Ground, MD 21005

8. PERFORMING ORGANIZATION REPORT NUMBER

DEVCOM DAC-TR-2022-033

9. SPONSORING / MONITORING AGENCY NAME(S) AND ADDRESS(ES)

10. SPONSOR/MONITOR'S ACRONYM(S)

11. SPONSOR/MONITOR'S REPORT NUMBER(S)

12. DISTRIBUTION / AVAILABILITY STATEMENT
DISTRIBUTION STATEMENT A. Approved for public release: distribution unlimited.

13. SUPPLEMENTARY NOTES

14. ABSTRACT
This study examined the trade-off between pelvis and lumbar-sacral spine (hereafter termed as spine or lumbar spine) injuries with simulated under-body blast loading applied to a seated Soldier posture in a military vehicle. The objectives were met by conducting postmortem human subject tests using a pelvis–lumbar spine experimental model.

15. SUBJECT TERMS
WIAMan, pelvis–lumbar fracture, loading trade-offs, under-body blast, UBB, PMHS, postmortem human subject

16. SECURITY CLASSIFICATION OF:			17. LIMITATION OF ABSTRACT	18. NUMBER OF PAGES	19a. NAME OF RESPONSIBLE PERSON
a. REPORT	b. ABSTRACT	c. THIS PAGE			Kathryn L. Loftis
UNCLASSIFIED	UNCLASSIFIED	UNCLASSIFIED	UU	59	19b. TELEPHONE NUMBER (include area code) (410) 306-0344

Table of Contents

Table of Contents

List of Figures

List of Tables

Executive Summary

A recent analysis comparing a theater injury dataset to component and whole-body human cadaver experiments, conducted for the Warrior Injury Assessment Manikin (WIAMan) project, showed that the fracture patterns to different body regions (pelvis, spine, etc.) were similar between the field and laboratory conditions. While whole-body cadavers produced injuries to pelvis and/or lumbar spine, the cited project did not explore biomechanical factors that may influence their injury patterns. The present study was designed to answer this question by identifying the time variable as a factor in the trade-off between pelvis and lumbar spine fractures (i.e., rate effect in the biological structure for the transmission of the vertical impact energy to the pelvis–lumbar subsystem). Based on theater, WIAMan whole-body and other human cadaver tests, it was hypothesized that pulses with short duration tend to bias the injuries to the pelvis while pulses that allow time (i.e., long duration) tend to bias to the spine, and as an extension, pulses in between these two categories (i.e., medium duration) tend to expose both the pelvis and spine components to injuries.

This concept was explored by examining the available WIAMan anthropomorphic test device (ATD) and whole-body data to develop parameters to define the targets for postmortem human subject (PMHS) experiments; 4 kN and 15 kN were chosen as the peak force level corresponding to ATD data for noninjury and injury loading, and 6 ms, 18 ms, and 36 ms were the targets for the short, medium, and long pulses for injury trade-off investigations. Using a repeated test protocol and WIAMan ATD, input parameters for the custom vertical accelerator device that applied the loading to PMHS specimens were obtained, and 12 PMHSs were used with a sample size of four for each pulse duration. The T12-pelvis specimens were prepared by attaching a load cell at the spinal end, aligned using the seated Soldier posture as the target, and impacted at the base using the vertical accelerator. Following the initial noninjury test, the specimen was palpated, radiographs were obtained, and upon confirming its integrity, the second injury loading test was conducted. After the test, X-rays and CT scans were obtained. Injuries were scored using the Abbreviated Injury Scale (AIS) version 2015, by a neuro-spine surgeon and a biomedical engineer, both authors of this report.

The mean age, stature, total body mass, body mass index, and lumbar spine bone mineral density (BMD) data were 64.8 ± 11.4 years, 1.8 ± 0.01 m, 83 ± 13 kg, 26.7 ± 5.0 kg/m^2, and 114.5 ± 21.3 mg/cc, respectively. The mean resultant forces corresponding to injury tests were 5.4 ± 1.5 kN, 5.3 ± 1.7 kN, and 5.9 ± 0.8 kN, respectively, for the short (target 5 ms), medium (target 17.5 ms), and long (target 35 ms) duration pulses. Specimen demographics and BMD data were not significantly different ($p<0.05$) for any combinations of pulses, and this was true for the axial, shear, and resultant forces, except shear force in one case. The lack of significance in the demographics, bone

quality, and forces suggests that the specimen selection and transmitted or absorbed force were not biased toward any pulse group—short, medium, or long. For the short pulse, two specimens sustained AIS 4, and one each sustained AIS 2 and AIS 3 severity injuries. For the medium pulse, two specimens each sustained AIS 3 and AIS 4 severity injuries, and for the long pulse, one specimen each sustained AIS 2 and AIS 4, and two sustained AIS 3 severity injuries.

These results confirm the hypothesis that long pulses bias injuries to the spine while short pulses bias to the pelvis (i.e., pelvis to spine injury trade-off increases with time). While not fully statistical, the study showed that the pelvis–lumbar spine subsystem response is dependent on the time factor of the application of the vertical impact load to the intact human cadaver pelvis. The time variable is, therefore, an appropriate candidate to consider for injury assessments, in conjunction with the force metric. Other candidates such as impulse, sustained force over a certain period, and rate of force application are examples for injury criteria that may better define or account for the trade-off issue.

1. INTRODUCTION

Injuries to vehicle-mounted warfighters during Operation Iraqi Freedom and Operation Enduring Freedom have been attributed to improvised explosive devices (IEDs).[1,2] When a vehicle is exposed to an IED from underneath, the event became referred to as under-body blast (UBB).[3–6] It is known that injuries can occur to the lumbo-pelvis complex from impact loadings.[3,5,7,8] Retrospective studies of combat-related events such as those from UBB events, compiled by international teams, have reported traumas to this complex and their importance to the safety of the Soldier and military mission.[2,3,9–13] Many studies have attributed the axially directed vector via the seat of the mounted Soldier/occupant to be a cause of injuries to these body regions from UBB and IEDs.[5,6,14–18]

Injury prevention strategies include the determination of the biomechanics of the complex under this vector. This is unique to the military, considering that automotive frontal or side impacts that occur in the horizontal plane do not usually involve this loading mode[19,20]. It is therefore necessary to understand the biomechanics of injuries to these body regions (pelvis and lumbosacral spine) under vertical impact loading. This was the goal of the Warrior Injury Assessment Manikin (WIAMan) project. Experiments were conducted with different types of human cadaver (postmortem human subject, PMHS) models. Whole-body and isolated pelvis and lumbar spine specimens were subjected to high-rate vertical loading at government and academic laboratories.[6,21–29] The cited references are not inclusive. Isolated pelvis UBB loading studies revealed differing injury patterns with different initial alignments: normal, anterior tilt, and posterior tilt.[22] Isolated lumbosacral spine studies under the same loading vector revealed compression-related fractures at different vertebral levels and with varying severities.[23,24,27] A recent analysis study compared a theater injury dataset to component and whole-body experiments, all conducted under the auspices of the WIAMan project.[30] Based on the Abbreviated Injury Scale (AIS) body regions (pelvis, spine, etc.), there was a similarity in the experimental and theatre fracture patterns. As expected, whole-body studies reported injuries to both body regions, some occurring in the same specimen.[6] Taken together, these studies produced lumbosacral spine and/or pelvis injuries in simulated UBB environments and replicated theatre trauma to the warfighter. The validity of these experimental models was established through these experiments.

As a composite system, injury to one body region or component affects the transmissibility of loads to the adjacent body region(s) as the human musculoskeletal components absorb and transmit the energy, and under the UBB loading vector, the transmissibility occurs from the pelvis to the sacral-lumbar spine. In other words, injuries sustained by the pelvis have implications in the energy transfer to the sacral-

lumbar spine. As fracture represents the state of, or implies, energy absorption, structural components cranial or superior to the injured component will sustain an altered state of mechanical loading (i.e., often less energy to be absorbed). Our previous whole-body human cadaver inferior-to-superior impact loading sled experiments showed the effect of acceleration pulse on migration of injuries to the pelvis–lumbar spine complex.[31] Specifically, intact PMHS tests were conducted by applying inferior-to-superior accelerations of different pulse shapes to the pelvis of a supine occupant. Although not statistical due to the limited sample size, longer pulses resulted in spine fractures while shorter pulses resulted in pelvis fractures. This was termed as mass recruitment effect on injury migration; in this case it was directed cranially. Changes in the rate of loading, reflected by the pulse shape, changed the injury pattern from the distal to the proximal regions of the specimen. This aspect could not be examined in the previous WIAMan project's isolated pelvis or lumbar spine experiments due to the lack of the spine or pelvic regions in these models. The issue of injury migration or trade-off between the two body regions, pelvis and/or lumbar spine, was the subject matter for our current WIAMan study.

2. OBJECTIVES

This study examined the trade-off between pelvis and lumbar-sacral spine (hereafter termed as spine or lumbar spine) injuries with simulated UBB loading applied to a seated Soldier posture in a military vehicle. The objectives were met by conducting PMHS tests using a pelvis–lumbar spine experimental model.

3. KEY QUESTIONS

Does a longer pulse induce spine injuries, does a shorter pulse induce pelvis injuries, and does a pulse in between the two durations induce both pelvis and spine injuries? What is the role of the peak loading, axial force, or resultant force, on injuries? To answer these questions, studies were conducted with the matched pair test protocol using WIAMan ATD and PMHS.

4. PART I: WIAMAN ATD STUDIES

4.1 Rationale for ATD studies

Matched pair testing protocol is an accepted methodology to replicate injuries and develop injury assessment reference curves (IARCs) in crashworthiness to advance human safety and improve vehicle designs. This has been followed in the automotive field for more than 70 years and is also true in the military. The matched pair design involves using the same conditions for the two surrogates, ATD and PMHS. In this case, for the lumbo-pelvis injury trade-off responses, the test conditions were based on lumbar loading observed in matched pair whole-body tests conducted by other performers. Lumbar loads from the matched pair ATD tests were obtained from its internal lumbar spine load cell. At the L5 level, a peak axial force of 15 kN in the dummy was associated with the lowest force that produced pelvic injuries in PMHS. A peak axial force of 4 kN was obtained from biofidelity response corridor tests for this dummy during its development, and it was based on matched pair PMHS tests in the earlier WIAMan project. For the current matched pair PMHS study, 4-kN and 15-kN force magnitudes, termed as noninjury and injury loads, were chosen as targets for noninjury and injury tests. Thus, tests with the ATD were planned at the three force magnitudes.

In the ATD lumbar axial force signals, time durations of 8–10 ms and 30–35 ms were the shortest and longest periods that corresponded with injuries to the pelvis and lumbar spine in PMHS whole-body tests, respectively. Hence, to investigate the trade-off issue, target pulse durations of 6 ms, 18 ms, and 36 ms were chosen to represent the short, medium, and long duration exposures.

The WIAMan pelvis–lumbar spine ATD experiments were conducted using the three pulses and three force levels. They were conducted to obtain the parameters for the vertical acceleration device (drop height and mass, energy absorbing material type and geometry, etc.) that were used as matched pair inputs to the PMHS specimens.

4.2 Methods

4.2.1 WIAMan ATD Preparation and Mounting to the Vertical Accelerator Loading Device

The ATD pelvis, pelvis skin, and lumbar spine components were affixed per normal configuration, and the abdominal insert was not included. The lumbar–pelvis assembly was mounted at the top of the spine to a carriage that translated vertically along a stanchion of the accelerator device (described later). The mount included a wedge that aligned the global x-z coordinates with a six-axis load cell (Model M3944, Sunrise

Instruments, Shanghai, China) on the spine and crosshairs on the pelvic skin. The ATD pelvis–lumbar spine along with its load cell at the superior end was attached to the custom vertical accelerator device that consisted of two components.[32] Figure 1 demonstrates the schematic of the device (left schematic shows the two sections). The impact component consisted of a stanchion fixed to the laboratory wall, a cart assembly, and a V-shaped lever arm attached to the seat platen. The drop-cart assembly allowed for vertical motion along the stanchion and weight adjustments. The cart mass was released with a predetermined height and impacted the lever arm, accelerating the specimen off the seat platen and up the free-standing impact-receiving component. This component allowed for positioning upon the seat platen and mounting of the superior end of the ATD to a cart and vertical track that constrained the preparation to post-impact vertical translation. An inspection was performed with rubber skin removed prior to and intermittently throughout testing sequence that consisted of repeated tests to achieve the goals: force and time duration levels, described earlier. The integrity of the internal pelvic components, lumbar lamination, and skin (rubber) abrasion at the impact site was examined during the testing process.

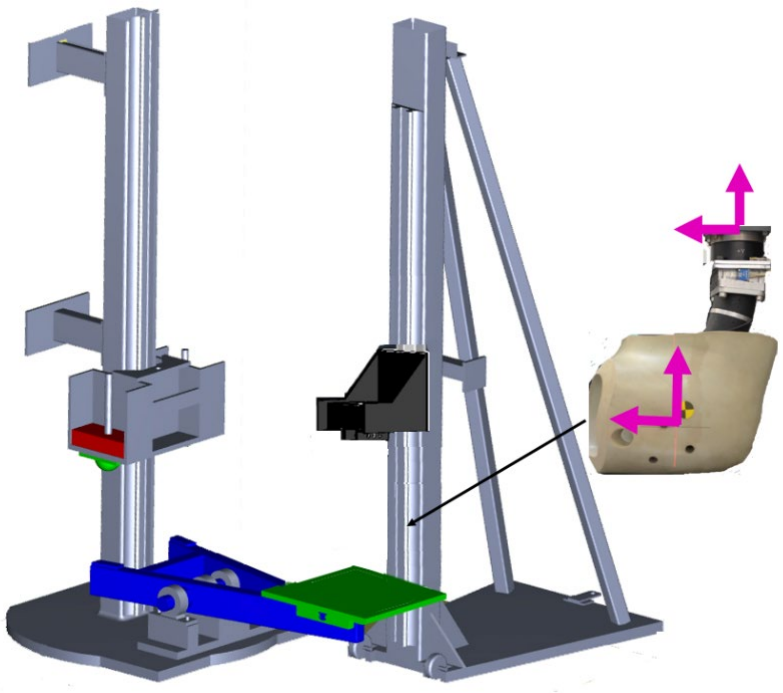

Figure 1. Schematic of the vertical accelerator (left with the two components), and WIAMan ATD. Arrows point to the x- (right-to-left) and z- (inferior-to-superior) axis. The load cell is shown on the top of the lumbar spine.

4.2.2 Test Protocol and Data Acquisition

Three repeated tests corresponding to peak 4-kN and 15-kN force magnitudes were conducted to achieve input parameters for each pulse duration. The vertical accelerator setup conditions from 18 tests served as inputs for the matched pair PMHS tests, with the recognition that tests corresponding to the 12 kN may be needed only if injury tests at 15 kN were found to be untenable for the PMHS. The ATD load cell data were acquired at a sampling rate of 100 kHz, force data was processed using a four-pole Butterworth low-pass filter at class 1000, and peaks and times of attainments were obtained to conform to the experimental design for the definition of the three pulses. Results from nine repeated tests are presented for the 15-kN tests as they formed the basis for the pelvis–spine injury trade-off investigations, the focus of this report.

4.3 Results and Discussion

The mean L5 axial force–time plots for the injury tests for the short, medium, and long pulses are shown in Figure 2. The input parameters that were used to set up the matched pair experiments are shown in Table 1. Details of the peak forces and their times of attainment are discussed in the next section.

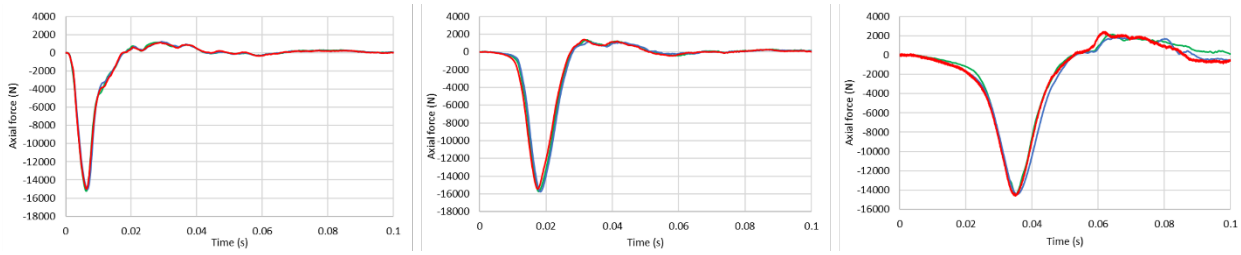

Figure 2. Repeated axial force signals for the short (left), medium (middle), and long (right) pulses

The objective of the ATD studies were to determine the input parameters for matched pair PMHS tests to investigate the trade-off issue. First, this was defined using lumbar spine axial forces from previous matched pair WIAMan ATD and whole-body tests that produced lumbar spine and/or pelvis injuries. As stated, at a force of 15 kN, pulses of 6 and 36 ms were considered to represent injuries to the pelvis and lumbar spine, respectively. The 17.5-ms medium-duration pulse was selected as the approximate midpoint between the short 6-ms and long 36-ms pulses. Targeting these pulses at 15 kN formed the injury test condition for matched pair PMHS test. As stated, a 4-kN force level was selected for the noninjury tests for these three pulses. As the trade-off studies are focused on investigating injuries in PMHS tests, plots of force–time responses for the noninjury ATD 4-kN tests are not reported. Data from the nine tests corresponding to the three pulses with three repeats were presented above, with all tests targeting the 15-kN magnitude.

For the short, medium, and long pulses, the mean coefficients of variation in the peak forces were 0.009, 0.011, and 0.006, respectively. The mean lumbar forces for these durations were 15.1 kN, 15.6 kN, and 14.5 kN, respectively, and the target was 15 kN. The somewhat lower force by approximately 0.5 kN for the long pulse was due to the introduction of the energy-absorbing material to extend the duration; however, the somewhat greater force by approximately 0.6 kN for the medium pulse was attributed to the lack of use of the padding material. Because both long and medium pulses deviated by approximately 0.5 kN, they were considered acceptable to conduct the PMHS tests for evaluating the trade-off issue.

The mean times of attainment of peak force for the short, medium, and long duration were 6.32 ms, 17.8 ms, and 35.1 ms, respectively, and the coefficients of variation were 0.004, 0.025, and 0.008, respectively. These data suggest that the setting used for these pulses adequately meets the targets. The low coefficient of variations demonstrated the repeatability of the WIAMan ATD to these test conditions and validated their use in similar situations. More than 100 tests were attempted with various iterations of parameters (shown in Table 1) to achieve the required targets of force and time.

The final PMHS test setup conditions from the described ATD testing are shown in Table 1 for each pulse. These data were used for the matched pair PMHS tests, and they are described in the next section. This completed the first part of the matched pair experimental protocol.

Table 1. Final PMHS Test Setup Conditions from ATD Testing

Pulse	Test Type	V-Arm	Drop Mass (kg)	Drop Height (m)	Stroke Adjustment	Top Pulse Shaper Material	Seat Cushion
Short	Noninjury	1:1	141	1.75	5/32-in. stroke; 0-in. rubber base	None	None
	Injury	1:1	168	2.48	29/32-in. stroke; 0-in. rubber base	None	None
Long	Noninjury	1:2	86	1.79	None	1-in. 50A rubber; 4-in. 2.0 PCF Ethafoam	None
	Injury	1:2	168	5.57	None	1-in. 50A; 4-in. XLPE 4.0 PCF polyethylene foam; 2-in. Ensolite SCC foam	4-in. 2.2 PCF Ethafoam
Medium	Noninjury	1:2	141	0.72	None	2-in. 50A rubber	None
	Injury	1:2	141	2.6	None	1.5-in. 70A; 2-in. 2.0 PCF Ethafoam	None

5. PART II: PMHS STUDIES

5.1 Rationale for PMHS Studies

With the described ATD studies serving as the framework for conducting matched pair PMHS tests, because of the non-frangibility of the ATD, PMHS experiments are necessary to investigate the trade-off issues between pelvis and spine, and they are applicable to the seated Soldier.

5.2 Methods

5.2.1 Specimen Preparation and Mounting

The protocol for human cadaver research was approved by the local institutional board and U.S. Army Human Research Protection Office. The experimental design consisted of isolating the full lumbar–pelvis subsystem from T11 to the acetabulum with musculature and abdominal skin, while removing the femora. PMHSs were screened to ensure no presence of blood-borne pathogens or spinal or pelvic abnormalities that may affect biomechanical injury outcomes. Pretest X-rays and computed tomography (CT) scans were obtained. The inclusion-exclusion criteria were such that all subjects were male, there were no surgical intervention to the lumbo-pelvis, there was no osteoporosis as determined by the quantitated CT bone mineral density (BMD) of the lumbar spine that followed the clinical guidelines (threshold 80 mg/cc), and there were no bridging osteophytes or congenital fusion of the spine–pelvis complex. The WIAMan inclusion-exclusion criteria were as follows: male-only specimens, 18 to 80 years, stature 165 to 186 cm, weight of 64 to 106 kg, and body mass index 18 to 35 kg/m^2.

While preparing the specimen, the contents of the pelvic bowl were removed; however, the ligamentous structures along the lumbar spinal column and within the pelvic ring were maintained intact. A cylindrical 11.5-kg ballistic gel form was contoured to fill the lower and upper abdominal cavities and to surround the lumbar spine. The pelvic angulation in the sagittal plane was targeted to be at a mean of 40° (standard deviation 5°). The orientation of 40° was defined as the angle of the pelvis plane with respect to the vertical axis.[33] The pelvis plane was defined as the lines connecting the bilateral anterior superior iliac spines with the pubic symphysis (Figure 3). The specimen was embedded in polymethylmethacrylate at the superior level. A six-axis load cell (Denton 3300 J; Humanetics Innovative Solutions, Farmington Hills, MI) was attached to the superior end of the fixation embedded in the T12 body. The specimens were aligned in a seated Soldier posture, according to a military study.[33] The cranial end of the specimen was manually flexed approximately 11.5° (standard deviation 5°) to achieve the posture.[33] A 2.7-kg and an 8.8-kg mass were added to represent the mass of the

pelvic and surrounding abdominal contents, and a mass of 12 kg was placed on the superior end of the preparation to account for the effective mass of the torso (Figure 3, mass shown in gray rectangle).[22] As stated, the pelvic mass was within the pelvic cavity, contouring the pelvic bowl from the rami inferiorly to the distal sacrum, and the abdominal mass was a cylindrical mold set atop the previous gel setting, surrounding the ilia and lumbar segments.

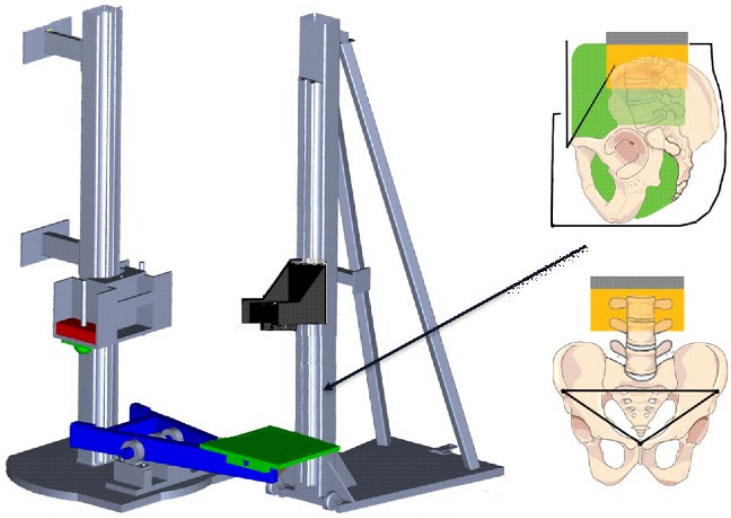

Figure 3. Schematic of the vertical accelerator (left with the two components), and specimen (showing the sagittal view in the middle and coronal views on the right). The load cell is shown as a shaded gray rectangle on top of the orange rectangle illustrating the added mass. The green shaded area shows the added surrounding abdominal mass.

5.2.2 Vertical Accelerator Loading Device

The custom vertical accelerator device used for ATD tests was also used for PMHS tests.[32] The details are repeated for completeness. The device consists of two components. Figure 3 demonstrates the schematic of the device (left schematic shows the two sections). The impact component consisted of a stanchion fixed to the laboratory wall, a cart assembly, and a V-shaped lever arm attached to the seat platen. The drop-cart assembly allowed for vertical motion along the stanchion and weight adjustments. The cart mass was released with a predetermined height and impacted the lever arm, accelerating the specimen off the seat platen and up the free-standing impact-receiving component. This component allowed for positioning upon the seat platen and mounting of the superior end of the specimen to a cart and vertical track that constrained the preparation to post-impact vertical translation. The mounting included a six-axis load cell affixed to the specimen potting, which constrained the superior end of the preparation.

5.2.3 Data Acquisition and Analysis

Sensor data were acquired at a sampling rate of 100 kHz, force and acceleration signals were processed using a four-pole Butterworth low-pass filter at class 1000. Load cell axial forces were compensated, representing the transmitted loads to the specimen. This paralleled the methodology used in the previous WIAMan project. Axial and shear forces in the sagittal plane and resultant force time histories were plotted injury tests for each specimen. Peak forces for each specimen were obtained, and statistical analysis of peak forces with pulse type was done using t-test.

5.2.4 Test Protocol, Imaging, and Injury Scoring

Pretest X-rays were obtained while the specimen was on the platform of the vertical accelerator to confirm the alignment. The experimental protocol was to conduct a noninjury and an injury test. After the first noninjury test at a nominal impact pulse that corresponded to the 4-kN ATD settings described in Table 1, the specimen was palpated, and X-rays were obtained to check the radiological integrity. The injury test was conducted next, at a greater impact level that matched the expected force level of 15 kN from matched-pair WIAMan ATD tests (Table 1 shows the settings). X-rays and CT scans were taken after the injury test. These data were used to identify and score the injuries. A practicing neuro-spine surgeon identified the injuries. They were scored using the Abbreviated Injury Scale, AIS 2015 version.[34] One AIS trained practicing clinician (JLB, an author of this report) and the other a certified AIS coder and biomedical engineer (KL, sponsor and author of this report) served as independent observers. Both were blinded to the test sequence and the association of the specimen identity with the type of injury test: short, medium, and long duration exposures.

5.3 Results and Discussion

5.3.1 General Data

The test matrix consisted of four specimens for each exposure type. The demographics of the 12 male specimens are displayed in Table 2: mean age, stature, total body mass, body mass index, and BMD data were 64.8 ± 11.4 years, 1.8 ± 0.01 m, 83 ± 13 kg, 26.7 ± 5.0 kg/m^2, and 114.5 ± 21.3 mg/cc, respectively. Appendix A shows the data on a specimen-by-specimen basis. Specimen demographics and BMD data were not significantly different ($p<0.05$, student t-test) in any combinations of pulses. The lack of significance in the demographics and bone quality suggests that the specimen assignment for the test was not biased toward any pulse group—short, medium, or long. All specimen data conformed to the exclusion-inclusion criteria, as described in the Methods section. From a segmental perspective, however, in one specimen the superior fixation failed and was re-fixed at the first lumbar vertebral level. The other two

specimens were shorter (PMHS 11 and 12), spanning from L1 to pelvis. These two specimens were used due to the time constraints and availability of the PMHS during the testing period. They were used for the final two medium pulse exposures. As described later, as both these specimens produced both spine and pelvis injuries even with a shorter column, in addition to proving the hypothesis of the involvement of both body regions with medium pulse exposure, it is likely that the injury outcomes would have been the same if the column was longer. This is because the longer column tends to show signs of failure due to increased slenderness. Additional experiments would be needed to reinforce these observations. They are future study topics.

Table 2. Specimen Data and Forces from Injury Tests

PMHS No.	Age (years)	Stature (cm)	Weight (kg)	Body Mass Index (kg/m^2)	Bone Mineral Density (mg/cc)
Mean	64.8	176.5	83.0	26.7	114.5
Std dev	11.4	5.7	13.1	5.0	21.3

5.3.2 Peak Forces

The peak axial, shear, and resultant forces for each specimen are given in Appendix A. The mean lumbar resultant forces were 5.6 kN, 5.9 kN, and 5.4 kN, respectively, for the short, long, and medium duration pulses (Table 3 shows the standard deviations). These data along with the axial and shear forces are given in Table 3. Figure 4 shows the axial, shear, and resultant forces for each duration type. Error bars show standard deviations. The axial, shear, and resultant forces were not significantly different ($p<0.05$) in any combinations of pulses, except shear force in one pulse combination (Table 4). The lack of statistical significance for the axial and resultant forces in addition to the randomized specimen selection show that the responses are not biased to the pulse type. The axial force is the major or principal resisting load under this mode, and axial forces exceeded the off-axis shear force, considered as a secondary component. The lack of statistical significance in the off-axis force in two out of three pulse combinations further reinforces the lack of bias in specimen selection for the test matrix. Additional samples should be tested in a future study to increase the robustness of these observations.

Table 3. Summary of Peak Force Results Based on Pulses

Parameter	Short Pulse	Long Pulse	Medium Pulse
Axial force (kN)	5.17 ± 0.91	4.55 ± 0.50	4.86 ± 1.61
Shear force (kN)	2.48 ± 0.76	3.82 ± 0.99	2.87 ± 1.26
Resultant force (kN)	5.57± 0.90	5.87 ± 0.94	5.35 ± 1.77

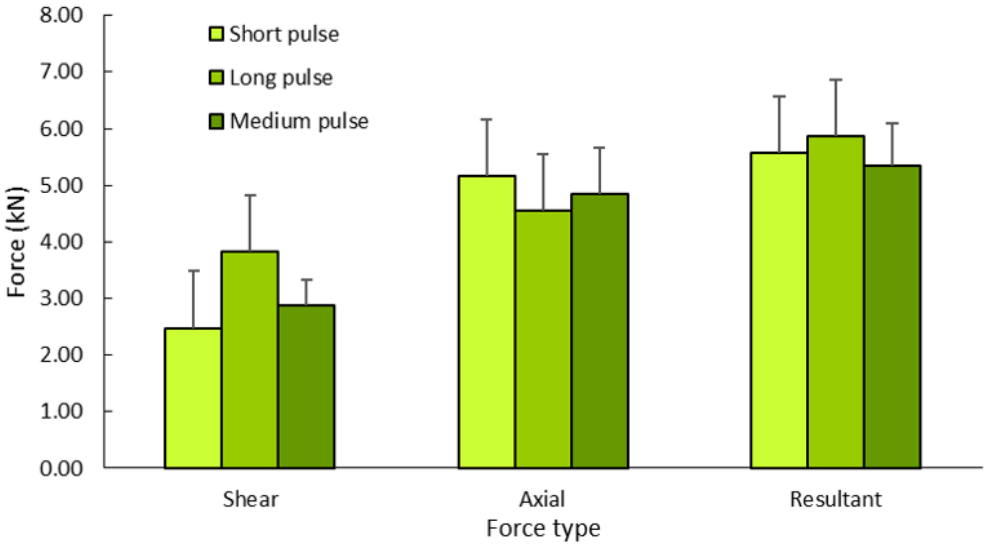

Figure 4. The axial, shear, and resultant forces for each duration type. Error bars denote standard deviations from a sample size of four PMHSs. Refer to text for details.

Table 4. Summary of p Values

Comparison of Pulses	Age	Height	Weight	BMI	BMD	Force		
						Axial	Shear	Resultant
Short vs. long	0.42	0.13	0.21	0.08	0.63	0.53	0.04	0.77
Medium vs. long	0.48	0.24	0.24	0.24	0.50	0.73	0.20	0.59
Short vs. medium	0.87	0.46	0.95	0.82	0.87	0.80	0.54	0.85

5.3.3 Injuries and AIS Levels

Appendixes B and C show the summary of injuries and AIS levels, and injuries on a specimen-by-specimen basis, respectively. Figure 5 shows the highest AIS (HAIS) levels for lumbar and/or pelvis injuries on a specimen-by-specimen basis. They are grouped into short, medium, and long pulses. They ranged between AIS 2 and AIS 4 for the entire ensemble. For the short pulse, there were two specimens in AIS 4, and one each in AIS 2 and AIS 3 severities. For the medium pulse, two specimens each were in AIS 3 and AIS 4 severities, and for the long pulse, there was one specimen in

each AIS 2 and AIS 4, and two in AIS 3 severities. Injuries at the fixation were not coded as it was attributed to, or influenced by, the rigidity of the specimen in the fixative material, and this occurred in specimen 2, associated with the long pulse. Likewise, the potential for cord injury was not included, as the neurological issue was deemed to be an inference rather than from the direct medical image readout from a PMHS test. A complete transection of the spine is unlikely in vivo because of the surrounding tissues and their tethering to the human lumbar spinal column, while the isolated lumbar PMHS column can transect due to the instability resulting from fracture. It should also be noted that bleeding issues cannot be included in PMHS experiments. Thus, injuries such as pelvis fractures that receive more severe scoring from AIS 4 to AIS 5 for the same structural injury cannot be replicated with this biological model, although it may be a relatively easier exercise to rescore or elevate the severity of some spinal injuries based on the bony encroachment space into the canal. This situation was applicable to specimens 6 and 10, with long and medium pulses.

A comparative evaluation of injuries based on AIS severities to the lumbar spine and pelvis is depicted in the form of bar charts in Figure 5. For the short pulse, pelvis injury severities were greater in three out of four cases/specimens, and in the other, both pelvis and lumbar spine had the same severity score of AIS 2 (i.e., one out of four cases). In addition, in one case (in the three out of four group), the spine injury was limited to AIS 1 (i.e., minor). These results confirm the proposed hypothesis that short pulses bias injuries to the pelvis and limit injuries to the spine to lower severities.

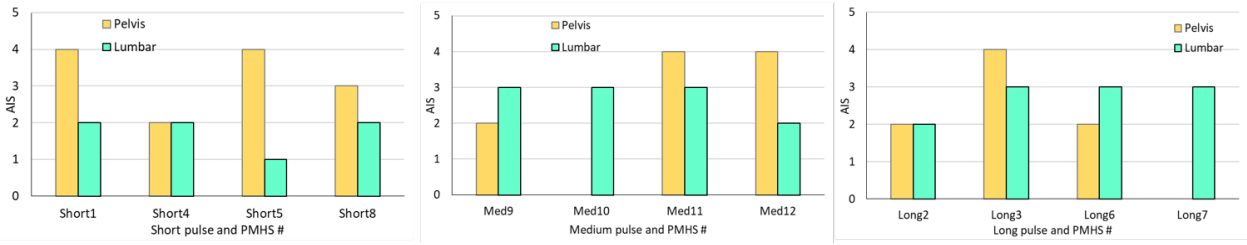

Figure 5. AIS levels for the spine and pelvis based on the short (left), medium (middle), and long (right) duration pulses. Example, Short1 refers to short pulse, specimen 1; Med9 refers to medium pulse, specimen 9; and Long2 refers to long pulse, specimen 2.

For the long pulse, all four specimens sustained AIS ≥2 injuries to the spine, and three of these sustained AIS 3 spine injuries. In contrast, there were only three specimens with pelvis injuries, out of which two had AIS 2 injuries, and one had AIS 4 fractures. These results confirm the trade-off toward spine injuries with the long pulse.

For the long pulse, one out of four specimens responded with lumbar spine–only injuries, the severity of lumbar spine injuries in three out of four specimens was greater than or equal to pelvis, and one specimen responded with a greater severity to pelvis than spine. This pattern is somewhat opposite to the short pulse and, with the limited

sample size, confirms the proposed hypothesis that long pulses bias injuries to the spine and limit injuries to the pelvis to lower severities. The issue of mass recruitment is discussed later.

For the medium pulse, in two cases pelvis injury severities were greater than spine injury severities, in one case the opposite was true, and in the other case there was only spine injury. The mixed nature of this pattern confirms the hypothesis that medium duration exposure leads to injuries to both regions albeit in a less expected manner.

In a more general manner, if AIS = 1 is excluded, the pelvis–spine injury counts were such that for the short pulse it was 4-3, medium pulse it was 3-4, and long pulse it was 3-4. The 4-3 to 3-4 switch from short to medium pulse appears to confirm the proposed concept of injury trade-off with the small size.

As another extension of this analysis, and considering that the previous WIAMan ATD outcomes in terms of IARCs were based on ignoring AIS = 1 for spine and AIS = 2 for pelvis (i.e., treating these injury severities as noninjury matched pair outcomes), the following observations are made. The outcomes for the short pulse would be three pelvis and three spine injuries; the medium pulse would be two pelvis and four spine injuries; and the long pulse would be one pelvis and four spine injuries. A more drastic drop-off of pelvis injury with increased duration is apparent from this analysis. This categorical assignment of injuries also supports the trade-off issue based on pulse duration.

Taken together, from testing four specimens in each case, these results confirm the role of the temporal variable in the trade-off between pelvis and spine injuries under vertical loading. As briefly stated in the introduction, the trade-off issue is due to the mass recruitment with time availability. This phenomenon was found to be true even in the current isolated PMHS testing environment. The absorption of the same transmitted resultant forces (insignificant difference at $p > 0.05$ level) in all specimens at the superior end of the spinal column fixation allowed to delineate the rate effect/pulse type on injury trade-off between the two body regions. The longer pulse allowing the mass of the inferior structures, in this case pelvis, to vertically accelerate placed an additional demand on the spinal column and exposed it to injuries. In contrast, the lack of the time availability in the short pulse exposed only the inferior or the immediately in-contact structure (i.e., pelvis) to the impact energy and resulted in biasing injuries to this region. Such effects may be more pronounced in a whole-body PMHS and in vivo situations.

Previous vertical loading lumbar spine tests were categorized into single and multilevel injuries.[23] It was therefore possible to evaluate spinal injuries based on pulse durations and the number of specimens sustaining those injuries from this perspective. Figure 6

shows the number of specimens with 1 and ≥1 level spinal injuries. They were further classified as (i) any spinal fracture that included body, disc, endplate, and/or transverse process-related injuries, and (ii) only body/disc, ignoring the endplate and transverse process-related injuries. The reason to omit the endplate and/or transverse process in the later definition is that they tend to be clinically insignificant in terms of treatment to the Warfighter. The AIS coding scheme allows scoring these relatively often minor fractures, with little impact to clinical treatment regimen, perhaps with a view to code all pathologies.[34] A more appropriate treatment-based scale such as incapacitation may be needed to improve the scoring of these injuries; this is a future study. As can be seen, for the former definition of injuries, more specimens with long pulses had most ≥1 level injuries, followed by medium and then short pulses. In the later definition, the hierarchy was long and medium with an equal number of specimens in each category and followed by the short pulse. These findings, albeit from a very limited sample size, show that the spinal injuries occur more frequently with medium and long pulses than short pulses, again confirming the general trade-off hypothesis even within the same body region.

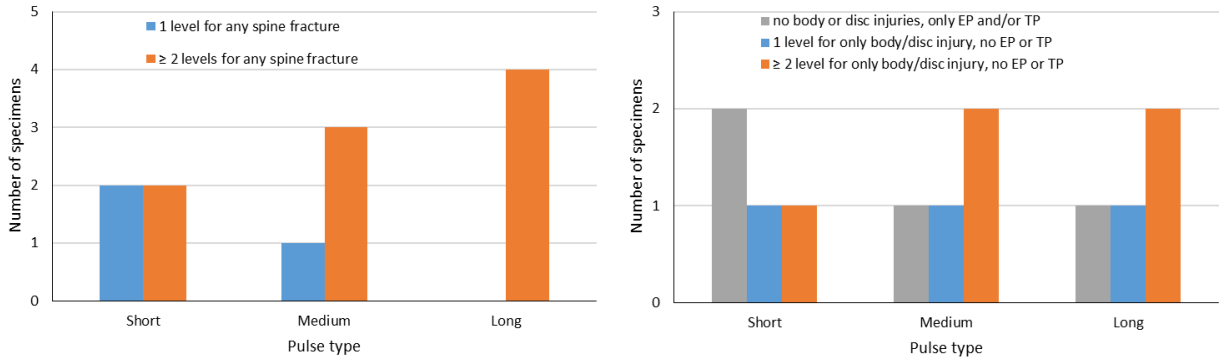

Figure 6. Number of specimens with single and ≥1 level injuries for the spine for the short, medium, and long duration pulses. Left bar chart shows the data for any spinal fracture and right bar chart shows the data with the exclusion of endplate and transverse process fractures, often considered clinically insignificant.

5.3.4 Limitations

The primary limitation is the sample size of four for each pulse case. While every effort was made to procure T12-pelvis specimens, time and inclusion-exclusion criteria constraints allowed all but two specimens with the full anatomical lumbar column: two were L1-pelvis. The sponsor approved the use of these two specimens before experimentation. While the use of the two specimens may appear to limit the applicability of the results, they were tested at the medium pulse and hence did not affect the primary outcomes of mass recruitment and trade-off between those that were focused on the pelvis and spine injuries (i.e., short and long pulses). In addition, as the outcomes from these two specimens appear to be congruent with the other two full

spinal column specimens, the conclusion regarding trade-off with respect to pulse timings is deemed tenable.

Likewise, while the target posture based on the seated Soldier study for the pelvis was achieved in all 12 specimens, it was not possible for the lumbar spine in 3 out of 12 specimens (PMHS 3, 4, and 6). This was due to their anatomy and joint flexibility, although they all met the inclusion-exclusion criteria. While the authors of this report do not believe that the outcomes would have been any different, additional specimens that fully comply with the seated Soldier posture angulations should be tested in the future. As posture plays a role in injuries, injury mechanisms, and tolerance, it may be important to study other initial alignments for the trade-off issue.

The generalizability to a larger population is an issue, as the exclusion-inclusion criteria were strict, and only male specimens were tested. While the trade-off issue has a basis in structural dynamics, because of differences in the pelvic anatomy between males and females, it would be necessary to test female specimens. The present matched pair experimental design can be used to achieve this objective. Data from female-specific spines will answer its trade-off issues; a comparison with male data may be used to better assess ATD outputs. Along these lines, computational models would be needed to determine segmental loads, and the present data can be used for validation. Pretest X-ray alignment and CT images can be used to develop PMHS-specific models and more accurately determine spinal loads.

As the practical application of the trade-off issue is to use the findings in IARCs, it may be important to develop human injury probability curves using these tests, perhaps considering them as a covariate and identify the optimal distribution that is most sensitive to, or best represents, the injury patterns and use the same PMHS-identified optimal function for the development of IARCs. Along the same vein, with more than one injury criteria candidate, it should be possible to use the Brier score metric (BSM) for ranking. The BSM is widely adopted in the WIAMan project. While these aspects were not the objectives and deliverables in the present statement of work, they need attention. Acknowledging these limitations, to fully test the hypothesis from a statistical perspective, the present limited sample study provides confidence in subjecting additional pelvis–spinal column specimens to vertical loading; this should be a future study topic. Appendix D provides time history plots of the resultant, axial, and shear force histories from injury tests for each specimen.

6. CONCLUSIONS

The test setup conditions from the ATD tests were used to conduct matched pair PMHS tests to examine the trade-off issue.

The PMHS study was designed to answer the questions regarding the trade-off between pelvis and spine injuries by including the rate effect (i.e., time variable in the experimental design). Based on previous theater and WIAMan whole-body and other human cadaver tests, it was hypothesized that pulses with short duration tend to bias the injuries to the pelvis while pulses that allow time (i.e., long duration) tend to bias to the spine, and as an extension, pulses in between the two categories (i.e., medium duration) tend to expose both the pelvis and spine to injuries. This was explored using the matched pair experimental design. The WIAMan ATD and whole-body data were used to develop parameters that defined the input parameters for PMHS experiments: 15 kN was chosen to be the peak force level based on ATD data, and 6 ms, 18 ms, and 36 ms were the targets for the short, medium, and long pulses for injury trade-off investigations. Using the repeated test protocol and ATD, the input parameters for the vertical accelerator were obtained, and 12 PMHS tests were conducted with a sample size of four for each pulse duration. While not fully statistical, the study showed that rate matters. Short duration affects pelvis injuries, long duration affects spine injuries, and medium durations affects injuries to both body regions. Thus, it appears that time variable is an appropriate candidate to consider for injury assessments, in conjunction with the peak force. Injury metrics such as impulse, sustained force over a certain period, and rate of force application are examples for the development of injury criteria that may better define, or account for, the trade-off issue.

7. REFERENCES

1. Owens, B. D., Kragh, J. F., Jr., Wenke, J. C., Macaitis, J., Wade, C. E., Holcomb, J. B. (2008). Combat wounds in Operation Iraqi Freedom and Operation Enduring Freedom. *J. Trauma, 64*(2), 295–299. doi: 10.1097/TA.0b013e318163b875 [published Online First: 2008/02/28]

2. Ramasamy, A., Harrisson, S. E., Clasper, J. C., Stewart, M. P. (2008). Injuries from roadside improvised explosive devices. *J. Trauma, 65*(4), 910–914. doi: 10.1097/TA.0b013e3181848cf6 [published Online First: 2008/10/14]

3. Loftis, K. L., Mazuchowski, E. L., Clouser, M. C., Gillich, P. J. (2019). Prominent injury types in vehicle underbody blast. *Mil. Med.*, *184*(Suppl 1), 261–264. doi: 10.1093/milmed/usy322 [published Online First: 2019/03/23]

4. Ramasamy, A., Masouros, S. D., Newell, N., Hill, A. M., Proud, W. G., Brown, K. A., Bull, A. M., Clasper, J. C. (2011). In-vehicle extremity injuries from improvised explosive devices: current and future foci. *Philos. Trans. R. Soc. Lond. B. Biol. Sci.*, *366*(1562), 160–170. doi: 10.1098/rstb.2010.0219 [published Online First: 2010/12/15]

5. Danelson, K., Watkins, L., Hendricks, J., Frounfelker, P., Team, W. I. C. R., Pizzolato-Heine, K., Valentine, R., Loftis, K. (2018). Analysis of the frequency and mechanism of injury to warfighters in the under-body blast environment. *Stapp Car Crash J, 62*, 489–513. [published Online First: 2019/01/05]

6. Danelson, K. A., Kemper, A. R., Mason, M. J., Tegtmeyer, M., Swiatkowski, S. A., Bolte, J. H. t., Hardy, W. N. (2015). Comparison of ATD to PMHS response in the under-body blast environment. *Stapp Car Crash J.*, *59*, 445–520. [published Online First: 2015/12/15]

7. Adams, S. A. (2009). Pelvic ring injuries in the military environment. *J. R. Army Med. Corps*, *155*(4), 293–296. doi: 10.1136/jramc-155-04-10 [published Online First: 2010/04/20]

8. Salzar, R. S., Bass, C. R., Kent, R., Millington, S., Davis, M., Lucas, S., Rudd, R., Folk, B., Donnellan, L., Murakami, D., Kobayashi, S. (2006). Development of injury criteria for pelvic fracture in frontal crashes. *Traffic Inj. Prev.*, *7*(3), 299–305. doi: 10.1080/15389580600660013 [published Online First: 2006/09/23]

9. Rankin, I. A., Nguyen, T. T., Carpanen, D., Clasper, J. C., & Masouros, S. D. (2020). A new understanding of the mechanism of injury to the pelvis and lower limbs in blast. *Front. Bioeng. Biotechnol.*, *8*, 960. doi: 10.3389/fbioe.2020.00960 [published Online First: 2020/09/10]

10. Spanos, I., Venetikidis, A., Zogopoulos, P., Vretakos, G., Rologis, D. (2016). Treatment of a patient with lumbosacral and pelvic fractures due to a blast injury

without surgical stabilization. *Clin. Case Rep. Rev.*, *2*(3), 358–360. doi: 10.15761/CCRR.1000217

11. Schoenfeld, A. J., Dunn, J. C., Bader, J. O., Belmont, P. J., Jr. (2013). The nature and extent of war injuries sustained by combat specialty personnel killed and wounded in Afghanistan and Iraq, 2003–2011. *J. Trauma Acute Care Surg.*, *75*(2), 287–291. doi: 10.1097/TA.0b013e31829a0970 [published Online First: 2013/07/28]

12. Schoenfeld, A. J., Laughlin, M. D., McCriskin, B. J., Bader, J. O., Waterman, B. R., Belmont, P. J., Jr. (2013). Spinal injuries in United States military personnel deployed to Iraq and Afghanistan: An epidemiological investigation involving 7877 combat casualties from 2005 to 2009. *Spine (Phila Pa 1976)*, *38*(20), 1770–1778. doi: 10.1097/BRS.0b013e31829ef226 [published Online First: 2013/06/14]

13. Spurrier, E., Gibb, I., Masouros, S., Clasper, J. (2016). Identifying spinal injury patterns in underbody blast to develop mechanistic hypotheses. *Spine (Phila Pa 1976)*, *41*(5), E268–75. doi: 10.1097/BRS.0000000000001213 [published Online First: 2015/11/17]

14. Helgeson, M.D., Lehman, R. A., Jr., Cooper, P., Frisch, M., Andersen, R. C., Bellabarba, C. (2011). Retrospective review of lumbosacral dissociations in blast injuries. *Spine (Phila Pa 1976), 36*(7), E469–75. doi: 10.1097/BRS.0b013e3182077fd7 [published Online First: 2011/03/02]

15. Kang, D. G., Cody, J. P., Lehman, R. A., Jr. (2012). Combat-related lumbopelvic dissociation treated with L4 to ilium posterior fusion. *Spine J.*, *12*(9), 860–861. doi: 10.1016/j.spinee.2011.05.017 [published Online First: 2011/07/19]

16. Patzkowski, J. C., Blair, J. A., Schoenfeld, A. J., Lehman, R. A., Hsu, J. R. (2012). Multiple associated injuries are common with spine fractures during war. *Spine J.*, *12*(9), 791–797. doi: 10.1016/j.spinee.2011.10.001 [published Online First: 2011/11/08]

17. Cross, A. M., Davis, C., Penn-Barwell, J., Taylor, D. M., De Mello, W. F., Matthews, J. J. (2014). The incidence of pelvic fractures with traumatic lower limb amputation in modern warfare due to improvised explosive devices. *J. R. Nav. Med. Serv.*, *100*(2), 152–156. [published Online First: 2014/10/23]

18. Yoganandan, N., Moore, J., Humm, J. R., Pintar, F. A., Banerjee, A., Baisden, J. L., Barnes, D. B., Loftis, K. L. (In press). Human pelvis injury risk curves from underbody blast impact. *BMJ* 2021.

19. National Highway Traffic Safety Administration. (2001). Frontal impact protection, FMVSS-208. 49 CFR § 571.214 - Standard No. 208 (2001).

20. National Highway Traffic Safety Administration. (2008). Side impact protection, FMVSS-214. 49 CFR § 571.214 - Standard No. 214. (2008).

21. Bailey, A. M., Christopher, J. J., Brozoski, F., Salzar, R. S. (2015). Post mortem human surrogate injury response of the pelvis and lower extremities to simulated underbody blast. *Annals of Biomedical Engineering*, *43*(8), 1907–1917. doi: 10.1007/s10439-014-1211-5 [published Online First: 2014/12/17]

22. Salzar, R. S., Spratley, E. M., Henderson, K. A., Greenhalgh, P. C., Zhang, J. Z., Perry, B. J., McMahon, J. A. (2020). The mechanical response and tolerance of the anteriorly-tilted human pelvis under vertical loading. *Annals of Biomedical Engineering*. doi: 10.1007/s10439-020-02634-6 [published Online First: 2020/09/26]

23. Yoganandan, N., Moore, J., DeVogel, N., Pintar, F., Banerjee, A., Baisden, J., Zhang, J. Y., Loftis, K., Barnes, D. (2020). Human lumbar spinal column injury criteria from vertical loading at the base: Applications to military environments. *J. Mech. Behav. Biomed. Mater.*, *105*, 103690. doi: 10.1016/j.jmbbm.2020.103690 [published Online First: 2020/04/14]

24. Yoganandan, N., Moore, J., Pintar, F. A., Banerjee, A., DeVogel, N., Zhang, J. (2018). Role of disc area and trabecular bone density on lumbar spinal column fracture risk curves under vertical impact. *J. Biomech.*, *72*, 90–98. doi: 10.1016/j.jbiomech.2018.02.030 [published Online First: 2018/03/22]

25. Sherman, D., Somasundaram, K., Begeman, P., Foley, S., Greb, J., Bir, C., Demetropoulos, C. K., Cavanaugh, J. M. (2021). Dynamic response of the thoracolumbar and sacral spine to simulated underbody blast loading in whole body post mortem human subject tests. *Annals of Biomedical Engineering*. doi: 10.1007/s10439-021-02753-8 [published Online First: 2021/03/17]

26. Somasundaram, K., Sherman, D., Begeman, P., Ciarelli, T., McCarty, S. A., Kochkodan, J. J., Demetropoulos, C. K., Cavanaugh, J. M. (2021). Mechanisms and timing of injury to the thoracic, lumbar and sacral spine in simulated underbody blast PMHS impact tests. *J. Mech. Behav. Biomed. Mater.*, *116*, 104271. doi: 10.1016/j.jmbbm.2020.104271 [published Online First: 2021/02/01]

27. Ortiz-Paparoni, M., Op 't Eynde, J., Kait, J., Bigler, B., Shridharani, J., Schmidt, A., Cox, C., Morino, C., Pintar, F., Yoganandan, N., Moore, J., Zhang, J., Bass, C. R. (2021). The human lumbar spine during high-rate under seat loading: A combined metric injury criteria. *Annals of Biomedical Engineering*. doi: 10.1007/s10439-021-02823-x [published Online First: 2021/07/24]

28. Demetropoulos, C., Cavanaugh, J., Ott, K., Rupp, J., Drewry III, D., Montoya, M., Barnes, D. B., Loftis, K. L. (2020). *Whole-body postmortem human subject (PMHS) testing technical report: Tests conducted in support of injury prediction capabilities development – test series WS10, WS11, and WS12* (Report No. CCDC DAC-TR-2020-040). CCDC Data & Analysis Center.

29. Demetropoulos, C., Ott, K., Drewry III, D., Montoya, M., Cavanaugh, J., Rupp, J., Barnes, D. B., Loftis, K. L. (2020). *Whole-body postmortem human subject (PMHS) injury outcome technical report* (Report No. CCDC DAC-TR-2020-048). CCDC Data & Analysis Center.

30. Danelson, K., Polich, J., Barnes, D., Bullock, G., Scott, A., Halvorson, J., O'Gara, T., Pilson, H., Babcock, S., Birkedal, J., McAllister, B, Loftis, K. (2021). Verification of high-rate vertical loading laboratory skeletal fractures by comparison with theater injury patterns. *Ann. Biomed. Eng.* https://doiorg/101007/s10439-021-02873-1

31. Yoganandan, N., Moore, J., Arun, M. W., Pintar, F. A. (2014). Dynamic responses of intact post mortem human surrogates from inferior-to-superior loading at the pelvis. *Stapp Car Crash J.*, *58*, 123–143. [published Online First: 2015/07/21]

32. Yoganandan, N., Pintar, F. A., Schlick, M., Humm, J. R., Voo, L., Merkle, A., Kleinberger, M. (2015). Vertical accelerator device to apply loads simulating blast environments in the military to human surrogates. *J. Biomech.*, *48*(12), 3534–3538. doi: 10.1016/j.jbiomech.2015.06.008 [published Online First: 2015/07/15]

33. Reed, M. P., Ebert, S. M. (2013, October 31). The seated soldier study: Posture and body shape in vehicle seats. https://pdfs.semanticscholar.org/f4f8/ad73a06bcebd6c97c2deff01dcdd57f5b2fb.pdf [accessed Feb 24, 2021].

34. AIS. Association for the Advancement of Automotive Medicine. (2015). The Abbreviated Injury Scale. In: AAAM, ed. American Association for Automotive Medicine.

Appendix A – Specimen Data and Forces from Injury Tests

PMHS No.	Age (years)	Stature (cm)	Weight (kg)	Body Mass Index (kg/m^2)	Bone Mineral Density (mg/cc)	Duration Type	Axial Force (kN)	Shear Force (kN)	Resultant Force (kN)
1	78.0	172.7	66.4	22.2	98.4	Short	3.8	2.0	4.0
2	63.0	185.4	76.4	22.2	115.2	Long	4.1	3.7	5.4
3	78.0	175.3	88.0	28.6	95.8	Long	4.3	4.2	6.0
4	67.0	175.3	95.0	30.9	96.4	Short	4.0	3.3	4.6
5	62.0	167.7	88.5	31.5	145.7	Short	5.5	1.9	5.8
6	42.0	170.0	107.0	37.0	120.8	Long	5.3	4.6	7.0
7	63.0	175.3	74.8	24.3	144.8	Long	4.5	2.7	5.1
8	46.0	177.8	99.1	31.3	125.5	Short	7.4	2.7	7.9
9	64.0	172.7	68.0	22.8	98.1	Medium	3.6	2.8	4.3
10	70.0	177.8	68.0	21.5	81.7	Medium	3.8	1.6	3.9
11	68.0	182.9	80.3	24.0	140.3	Medium	7.0	2.9	7.4
12	77.0	185.4	84.1	24.5	111.0	Medium	5.2	4.2	5.8
Mean	64.8	176.5	83.0	26.7	114.5				
Std dev	11.4	5.7	13.1	5.0	21.3				

Appendix B – Injuries and Abbreviated Injury Scale Levels

PMHS	Anatomy/level	injury	AIS 2015 Version	HAIS lumbar	HAIS pelvis	HAIS
1	L2	L2 endplate fractures, inferior and superior	650630.2	2	4	4
	Sacrum	Bilateral sacral ala fractures, right displaced	856171.4			
		Bilateral sacral ala fractures left non-displaced				
		Zone 2 L sacral fracture				
		Transverse S5 process fracture				
	Pubis	Right Superior ramus-displaced fracture				
		Right body near pubic symphysis, inferior ramus, nondisplaced fracture				
	SI Joint	Inferior right SI diastasis with right sacral alar fracture				
2	L2 right	Transverse process fracture	650620.1	2	2	2
	L3 right	L3 bilateral trans process fracture	650620.1			
	L3 left	L3 bilateral trans process fracture	650620.1			
	L5	L5 Superior and inferior endplate fracture	650630.2			
	Sacrum	Transverse nondisplaced SC joint	856151.2			
3	T12-L1	Bilateral pars fracture, right	650426.2	3	4	4
		Bilateral pars fracture, left	650426.2			
		T12-L1 facet dislocation	650412.3			
	L1	Burst fracture	650636.3			
	L2	Burst fracture	650636.3			
	Sacrum	S2 horizontal fracture, S2-3, S1-S2 facet fracture	856171.4			
		Sacral ala bilateral fracture				
		S1 zone 1 and 2, S2 zone 1-2-3, S3 zone 2-3 fracture				
	ischium (right)	ST ligament incomplete tear				
	SI Joint	Left SI comminuted with left sacral ala fracture				
4	L3	L3 Compression fracture with sup endplate, <20% height loss	650632.2	2	2	2
	L4	L4 Compression fracture with sup endplate, <20% height loss	650632.2			
	Sacrum	Sacrococcygeal fracture	856151.2			
5	L5	Right transverse process fracture	650620.1	1	4	4
	Sacrum	S1 - alar and zone 2 fracture	856171.4			
		S2 - alar and zone 2,3 f fracture x				
		Bilateral Posterior arch fracture				
	Ischium (right)	Ischial tuberosity fracture				
6	L1	L2 Compression fracture with sup endplate, <20% height loss	650620.2	3	2	3
	L2-3	Disc rupture	650605.3			
	L3	Minor compression fracture superior endplate	650632.2			
	Sacrum	Anterior proximal to SC joint	856101.2			
7	T12-L1	Disc rupture	650605.3	3	0	3
	L1	Compression and sup EP, <20% height loss	650632.2			
	L3	Burst 3 column fracture	650636.3			
8	L1	Superior endplate fracture <20% height loss	650632.2	2	3	3
	L5	Right transverse process fracture	650620.1			
	sacrum	Bilateral alar zone 1 fracture	856161.3			
		S2-3 zone 3 fracture				
		Body fracture				
9	L1	Compression fracture L1 with sup endplate <20% height loss	650632.2	3	2	3
	L2	Burst 3 column fracture and retropulsion	650636.3			
	S5 + coccyx	Transverse fracture	856151.2			
10	T12-L1	T12-L1 fracture dislocation	610428.3	3	0	3
11	L1-2	Disc rupture	650605.3	3	4	4
	L3	Superior endplate fracture <20% height loss	650632.2			
	L5	Bilateral transverse process fracture - right	650620.2			
	L5	Bilateral T transverse process fracture - left	650620.2			
	Sacrum	Left S1 ala and zone 2. S2 ala and zone 2, S3 Zone2-3S1-3 bilat	856171.4			
	pubis	symphysis -nondisplaced fracture				
	SI joint	Minimal involvement with left sacral ala fracture				
12	L2	L2 superior endplate and <20% compression fracture	650632.2	2	4	4
	sacrum	Bilateral alar fracture Zone2, and zone 3 fracture bilat S1-2-3	856171.4			

Appendix C – Injuries for Each Specimen

See Appendix B for descriptions of injuries and Abbreviated Injury Scale levels.

PMHS 1: Images showing injuries

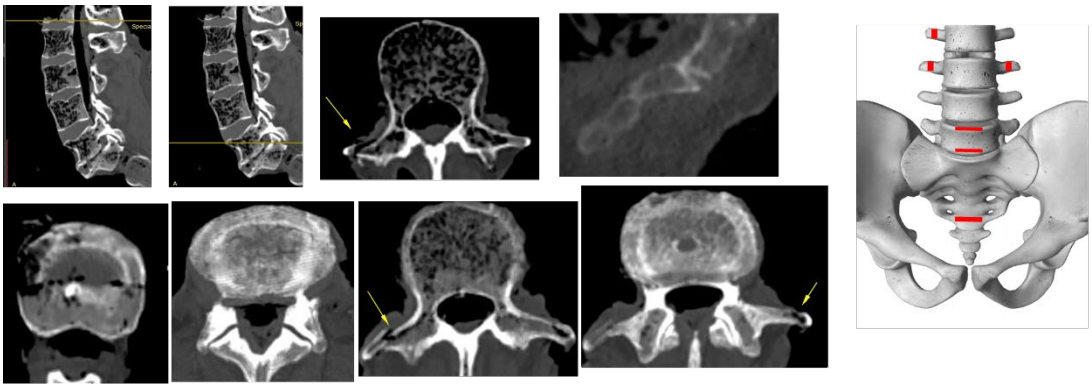

PMHS 2: Images showing injuries

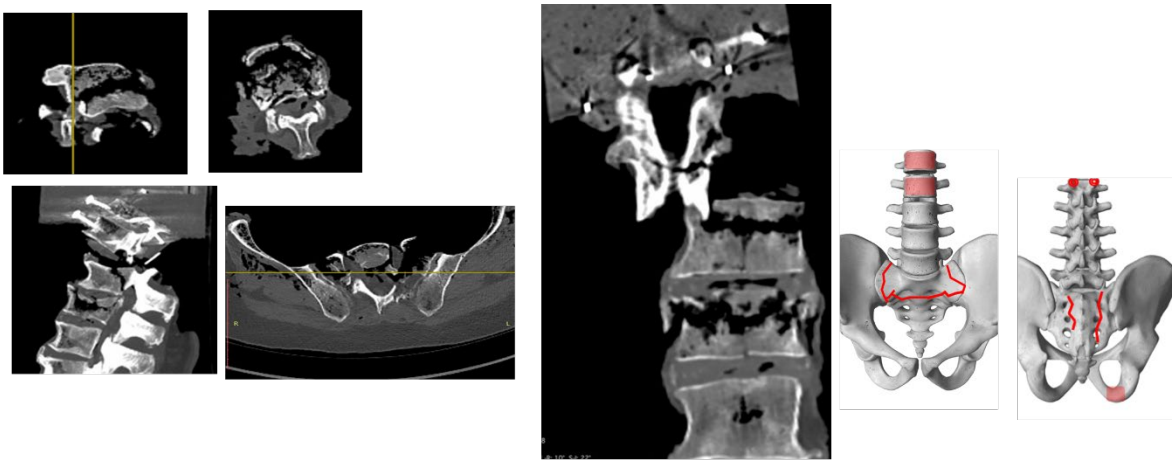

PMHS 3: Images showing injuries

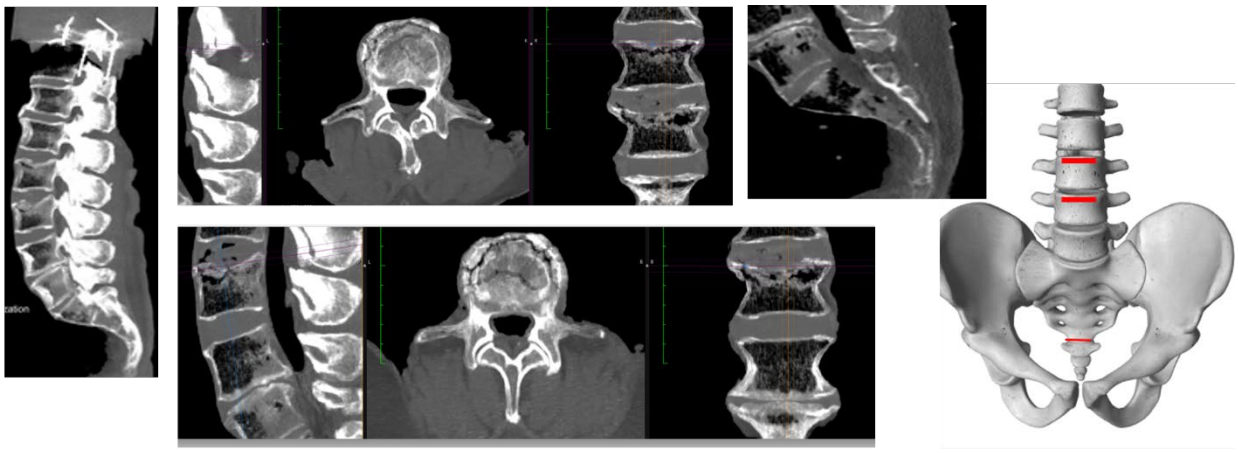

PMHS 4: Images showing injuries

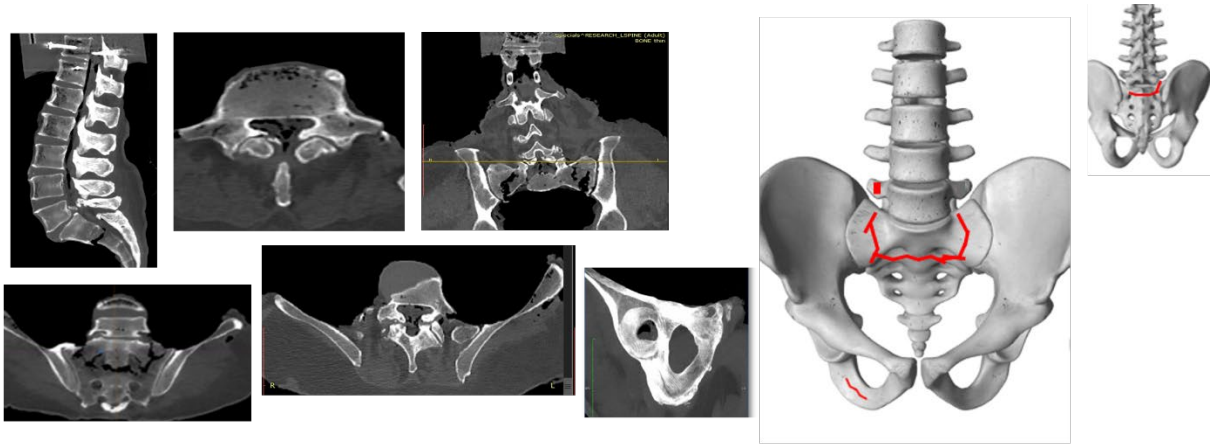

PMHS 5: Images showing injuries

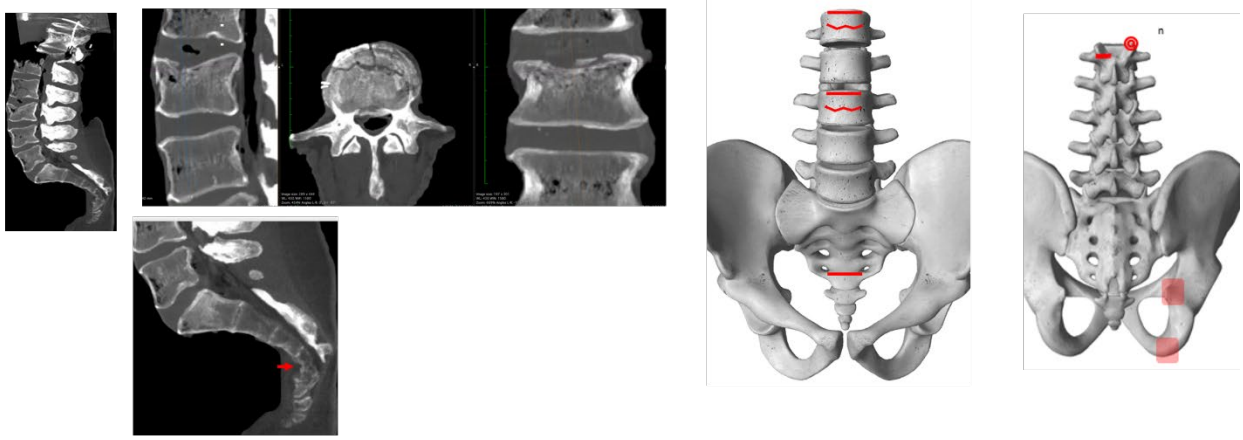

PMHS 6: Images showing injuries

PMHS 7: Images showing injuries

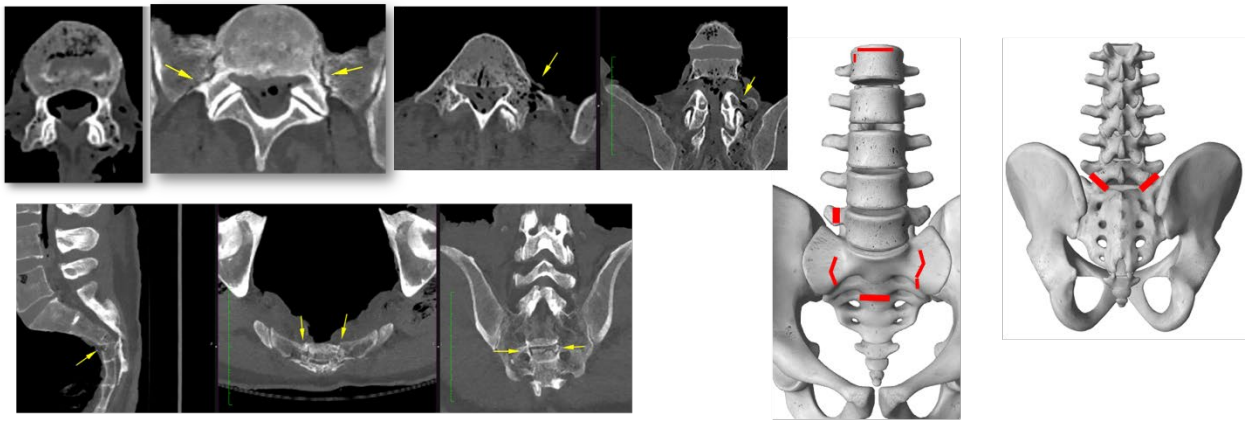

PMHS 8: Images showing injuries

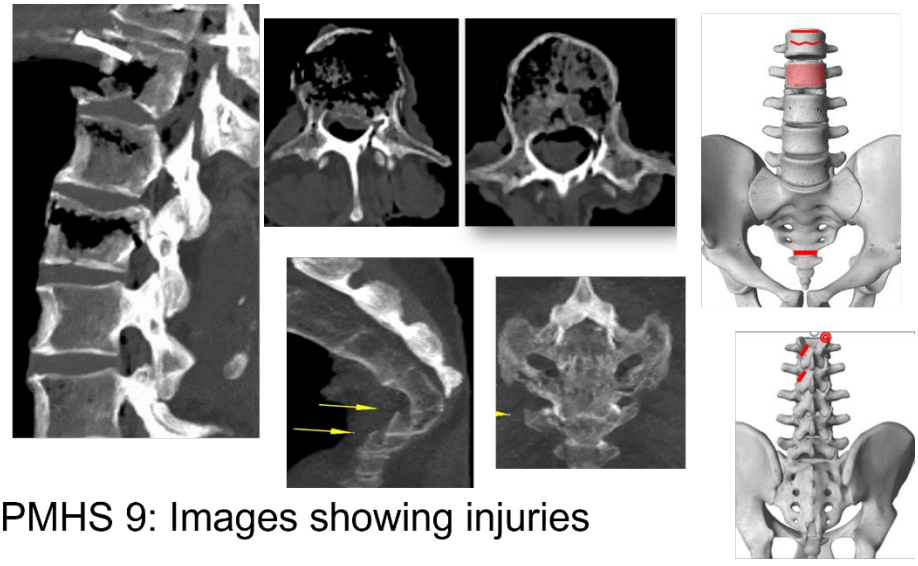

PMHS 9: Images showing injuries

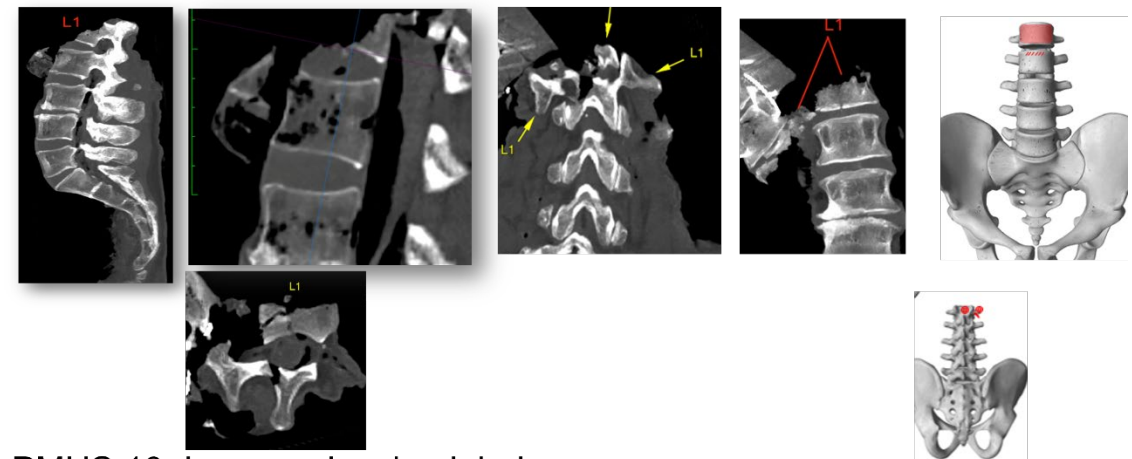

PMHS 10: Images showing injuries

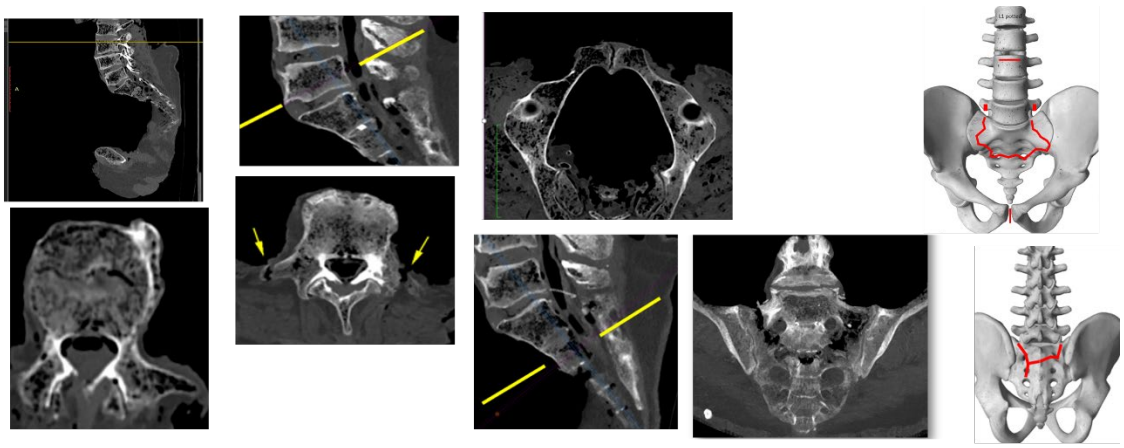

PMHS 11: Images showing injuries

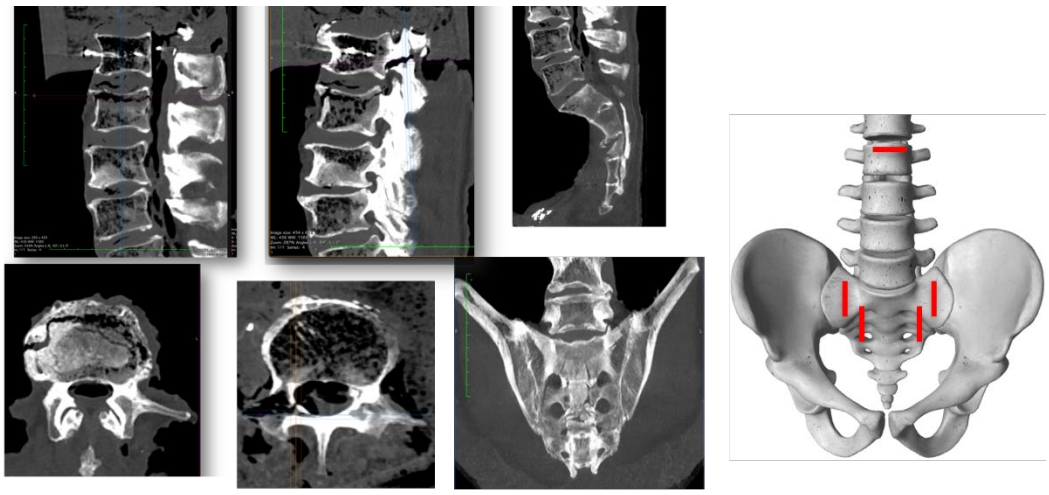

PMHS 12: Images showing injuries

Appendix D – Resultant, Axial, and Shear Force Histories from Injury Tests for Each Specimen

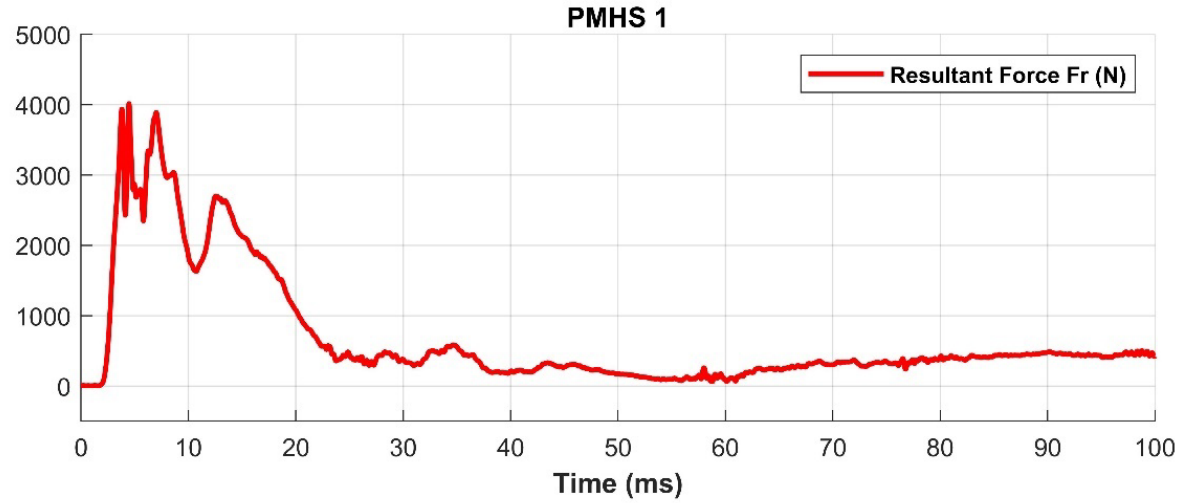
PMHS 1
Resultant Force Fr (N)
5000
4000
3000
2000
1000
0
0
10
20
30
40
50
60
70
80
90
100
Time (ms)

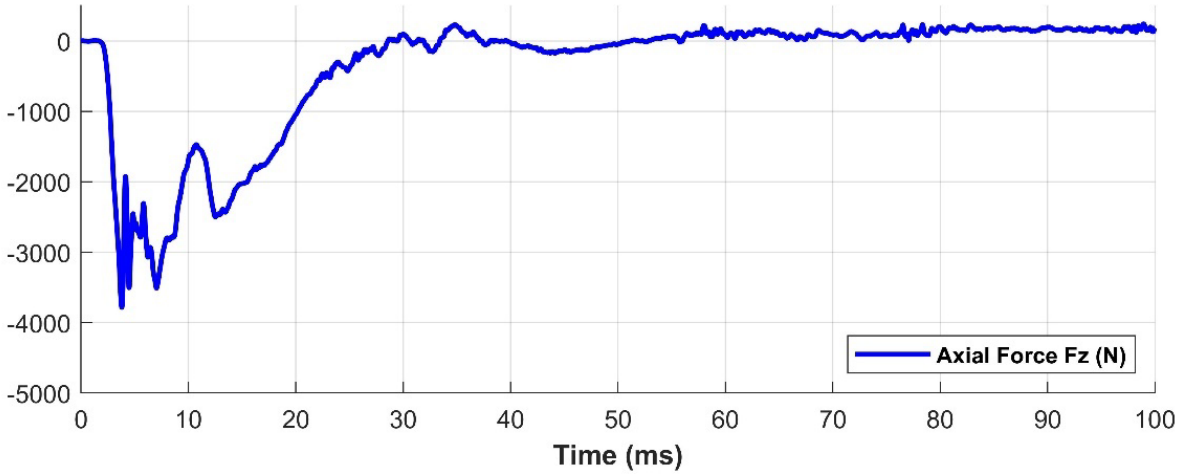
0
-1000
-2000
-3000
-4000
-5000
Axial Force Fz (N)
0
10
20
30
40
50
60
70
80
90
100
Time (ms)

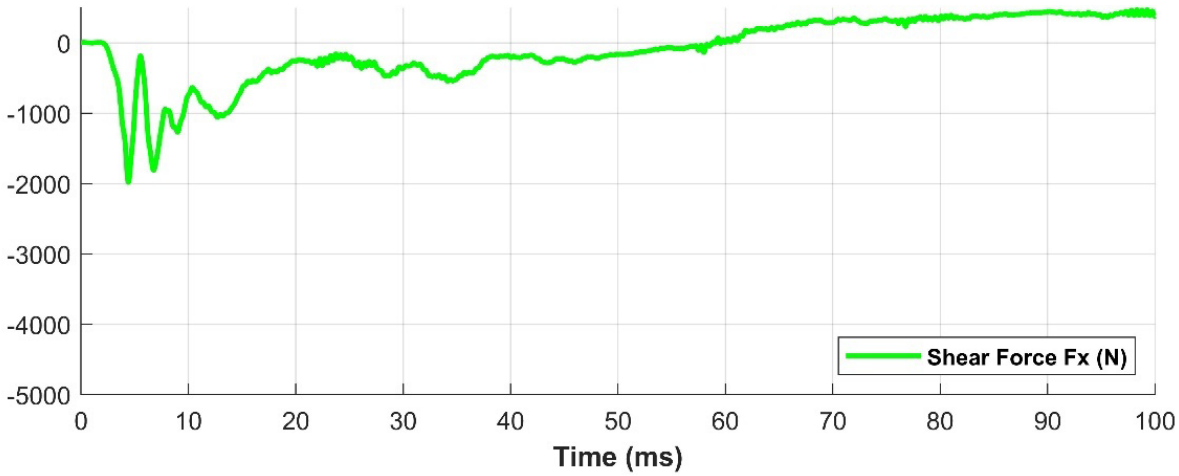
0
-1000
-2000
-3000
-4000
-5000
Shear Force Fx (N)
0
10
20
30
40
50
60
70
80
90
100
Time (ms)

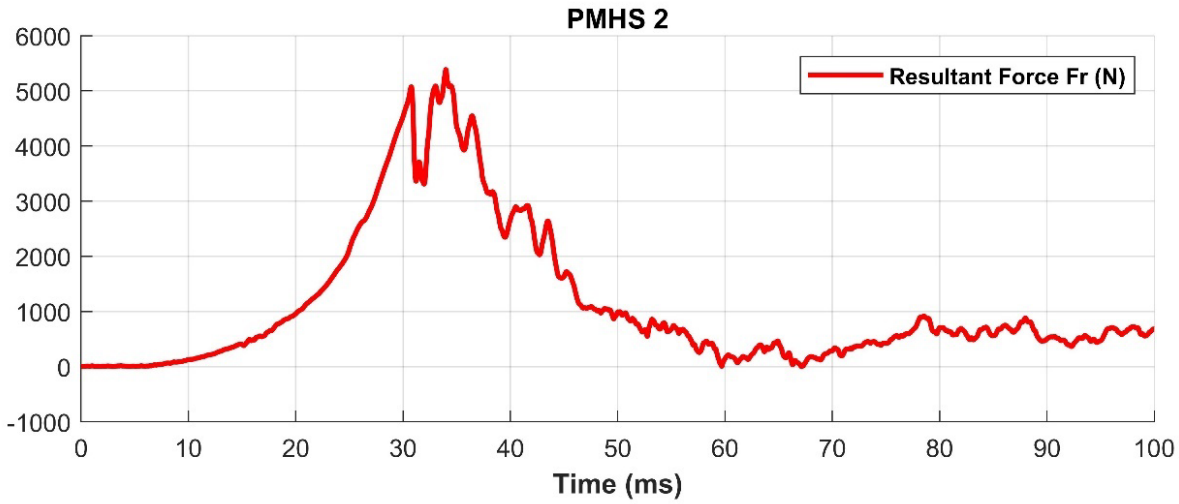
PMHS 2
Resultant Force Fr (N)
6000
5000
4000
3000
2000
1000
0
-1000
0
10
20
30
40
50
60
70
80
90
100
Time (ms)

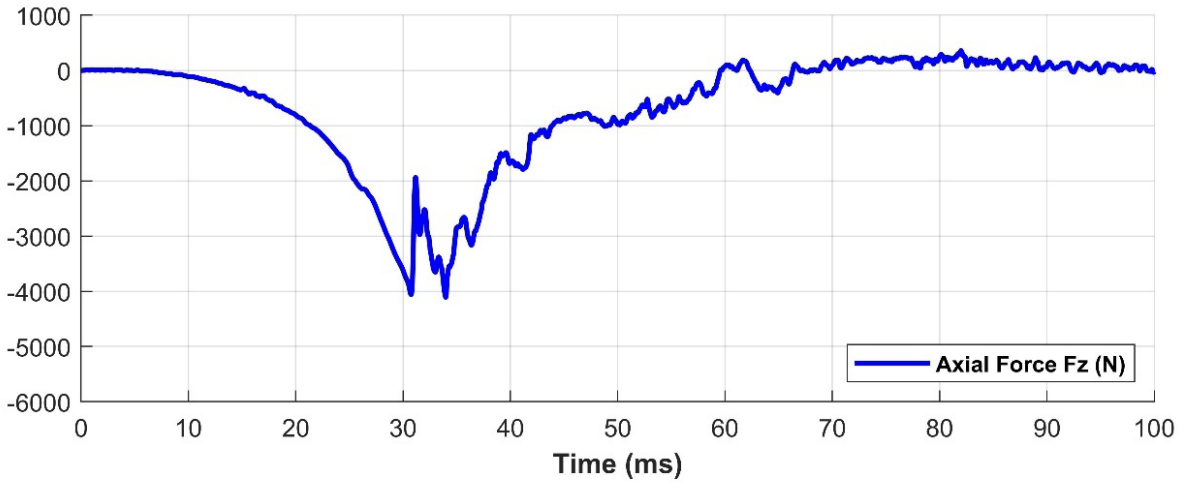
1000
0
-1000
-2000
-3000
-4000
-5000
-6000
Axial Force Fz (N)
0
10
20
30
40
50
60
70
80
90
100
Time (ms)

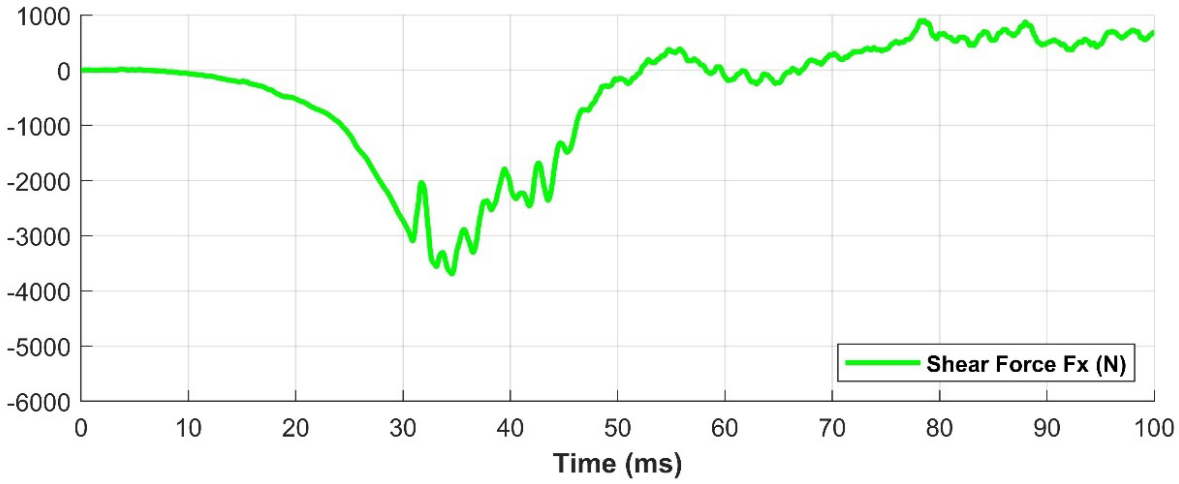
1000
0
-1000
-2000
-3000
-4000
-5000
-6000
Shear Force Fx (N)
0
10
20
30
40
50
60
70
80
90
100
Time (ms)

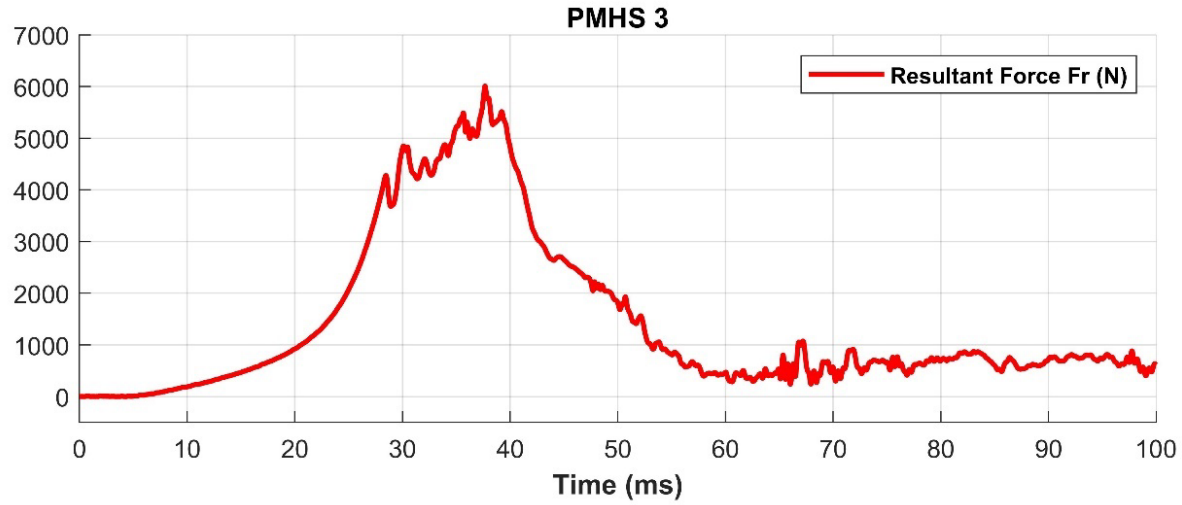
PMHS 3
Resultant Force Fr (N)
7000
6000
5000
4000
3000
2000
1000
0
0
10
20
30
40
50
60
70
80
90
100
Time (ms)

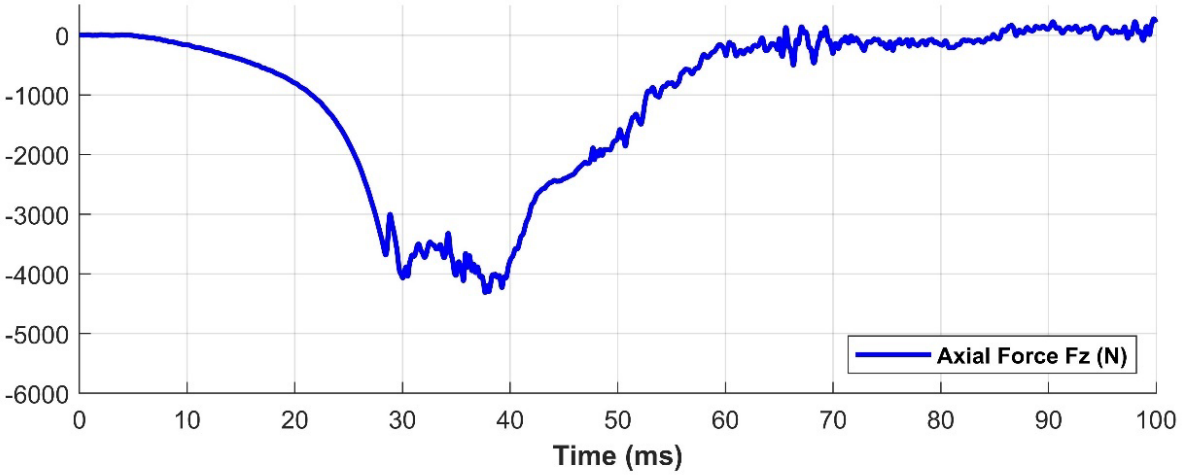
Axial Force Fz (N)
0
-1000
-2000
-3000
-4000
-5000
-6000
0
10
20
30
40
50
60
70
80
90
100
Time (ms)

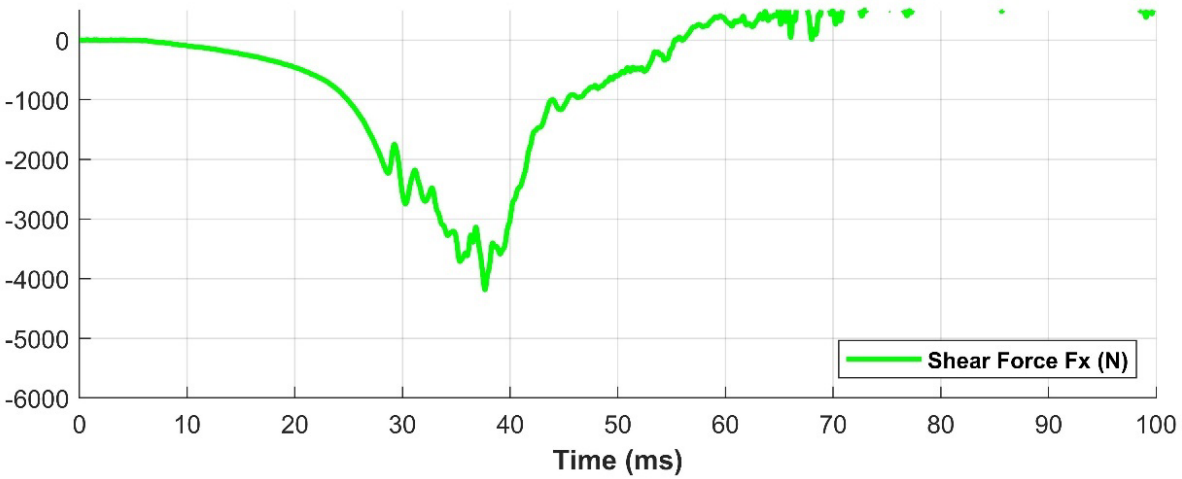
Shear Force Fx (N)
0
-1000
-2000
-3000
-4000
-5000
-6000
0
10
20
30
40
50
60
70
80
90
100
Time (ms)

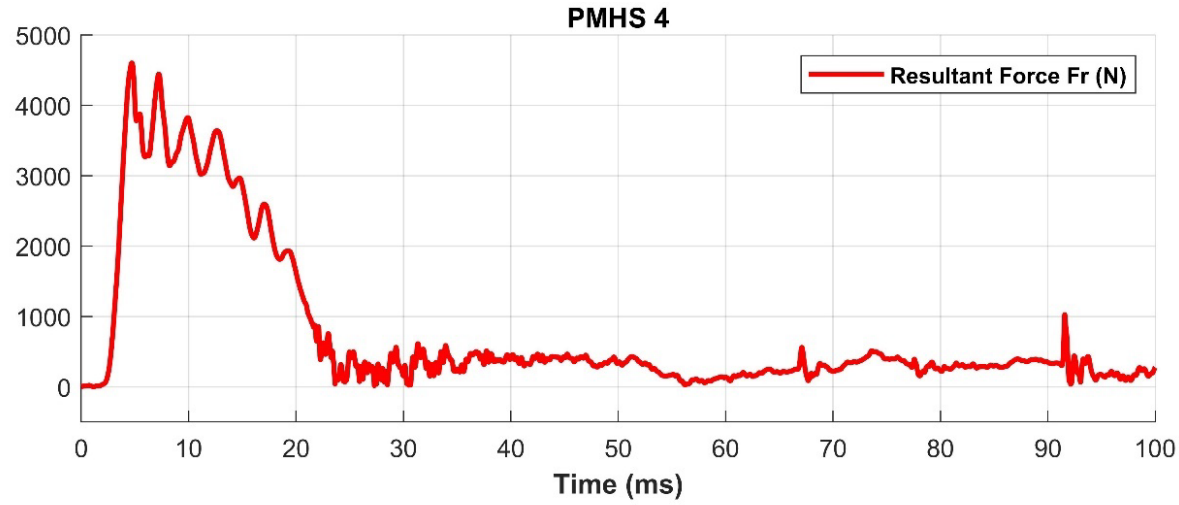
PMHS 4
Resultant Force Fr (N)
5000
4000
3000
2000
1000
0
0
10
20
30
40
50
60
70
80
90
100
Time (ms)

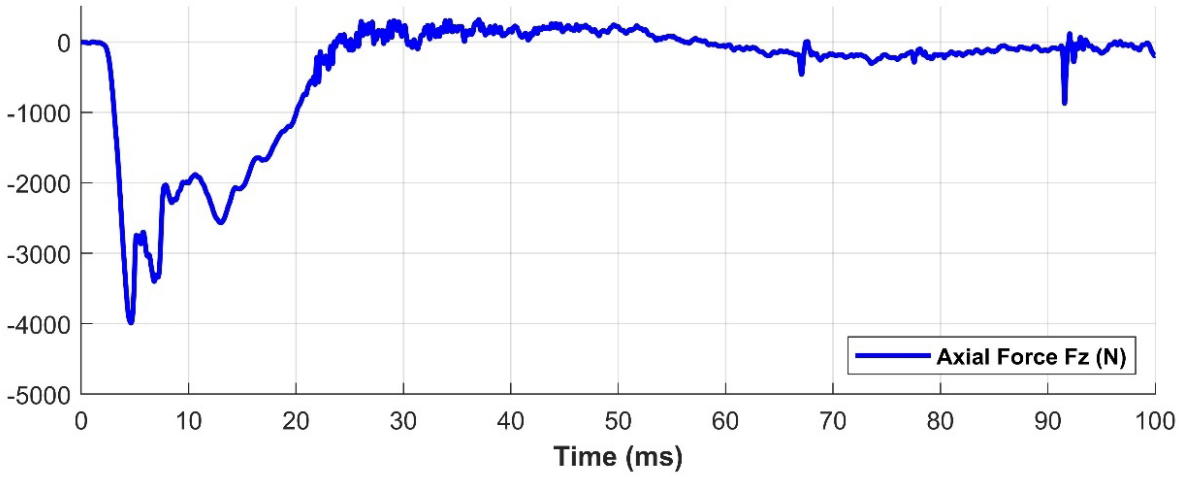
0
-1000
-2000
-3000
-4000
-5000
Axial Force Fz (N)
0
10
20
30
40
50
60
70
80
90
100
Time (ms)

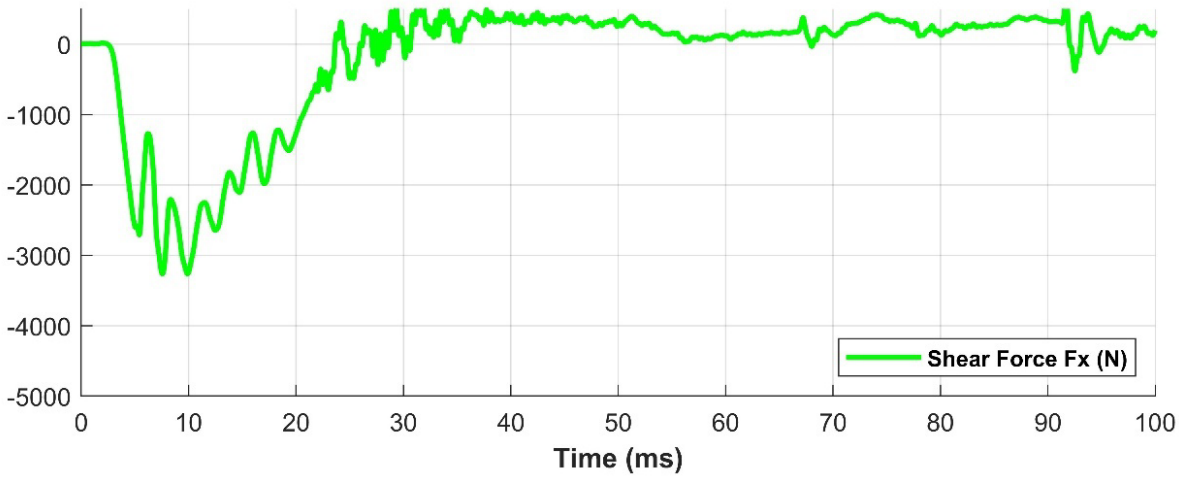
0
-1000
-2000
-3000
-4000
-5000
Shear Force Fx (N)
0
10
20
30
40
50
60
70
80
90
100
Time (ms)

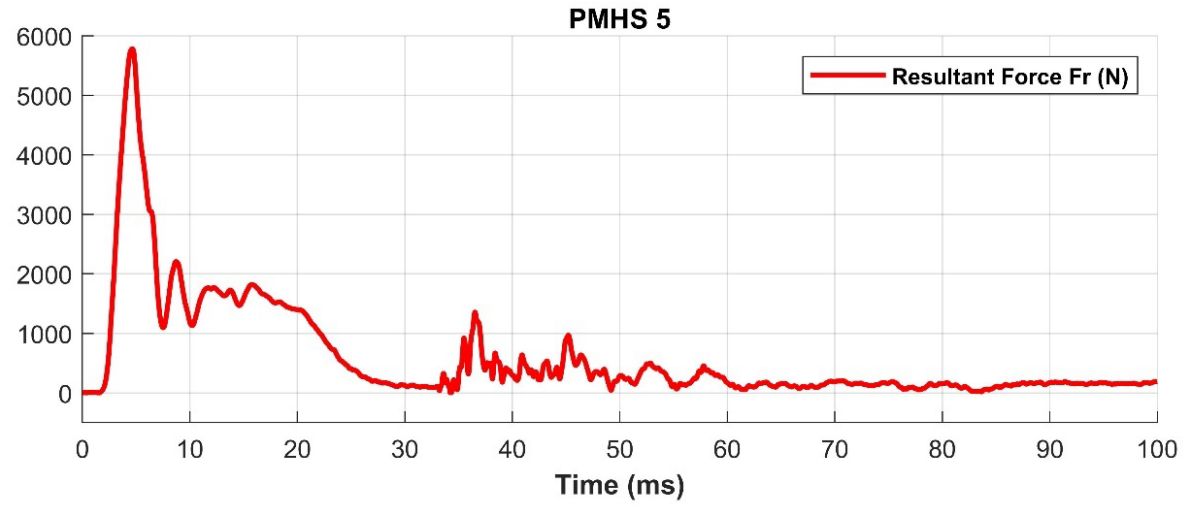
PMHS 5
Resultant Force Fr (N)
6000
5000
4000
3000
2000
1000
0
0
10
20
30
40
50
60
70
80
90
100
Time (ms)

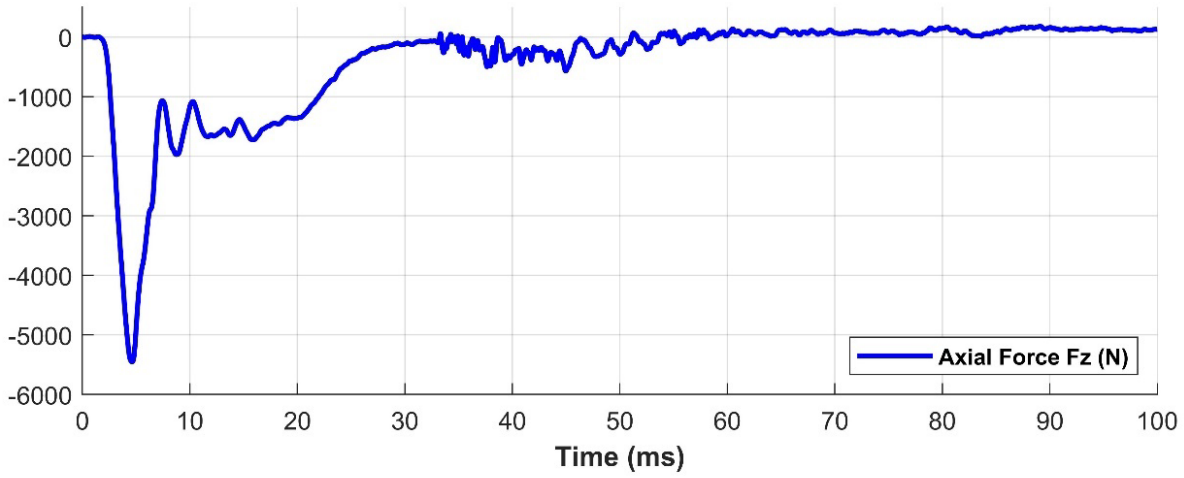
0
-1000
-2000
-3000
-4000
-5000
-6000
Axial Force Fz (N)
0
10
20
30
40
50
60
70
80
90
100
Time (ms)

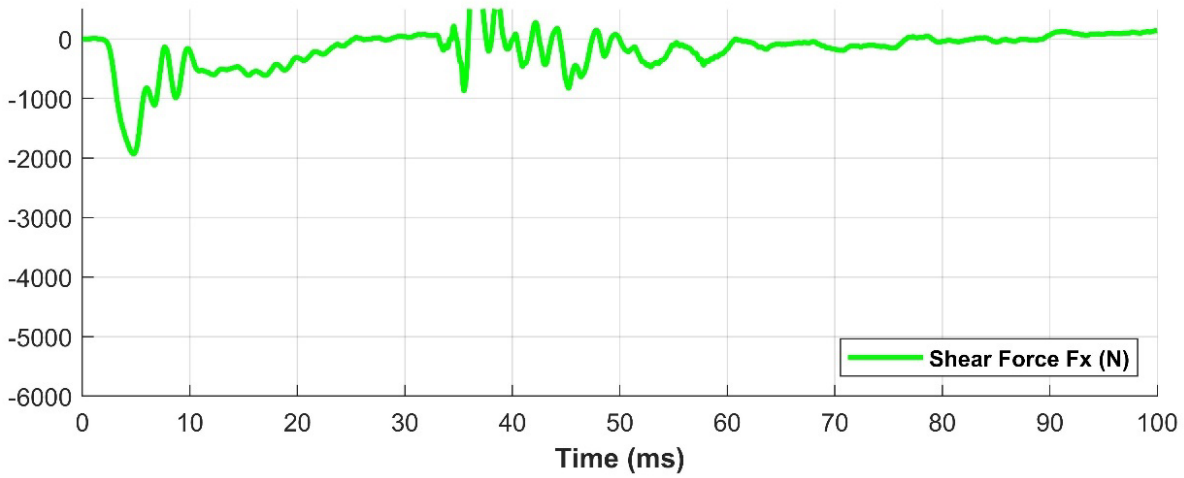
0
-1000
-2000
-3000
-4000
-5000
-6000
Shear Force Fx (N)
0
10
20
30
40
50
60
70
80
90
100
Time (ms)

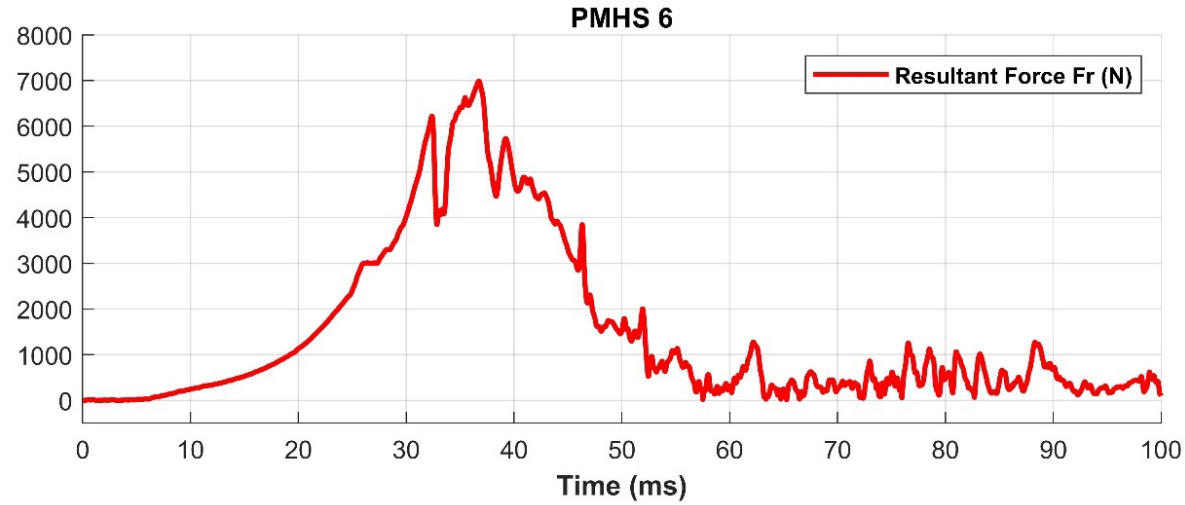
PMHS 6
Resultant Force Fr (N)
8000
7000
6000
5000
4000
3000
2000
1000
0
0
10
20
30
40
50
60
70
80
90
100
Time (ms)

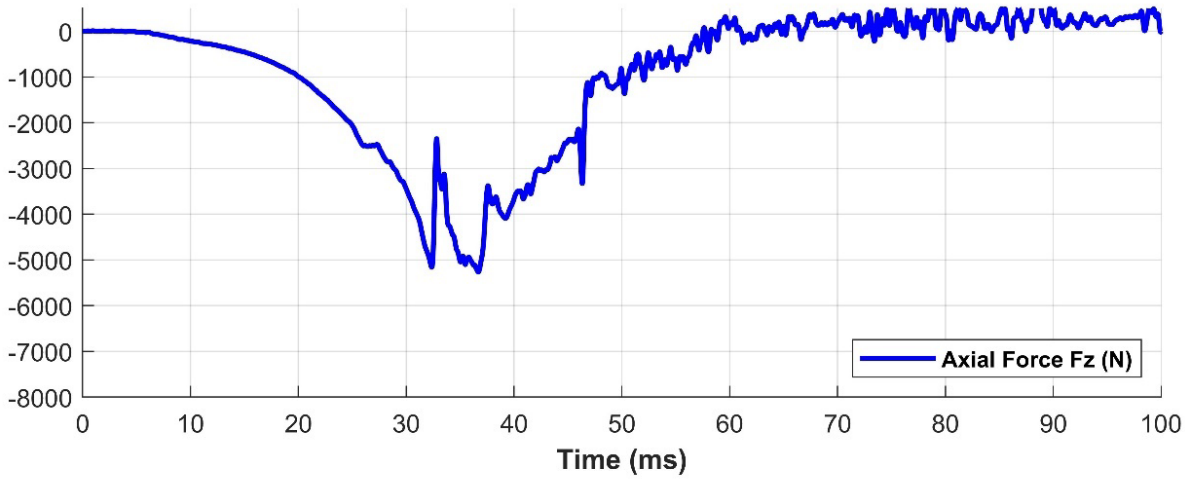
Axial Force Fz (N)
0
-1000
-2000
-3000
-4000
-5000
-6000
-7000
-8000
0
10
20
30
40
50
60
70
80
90
100
Time (ms)

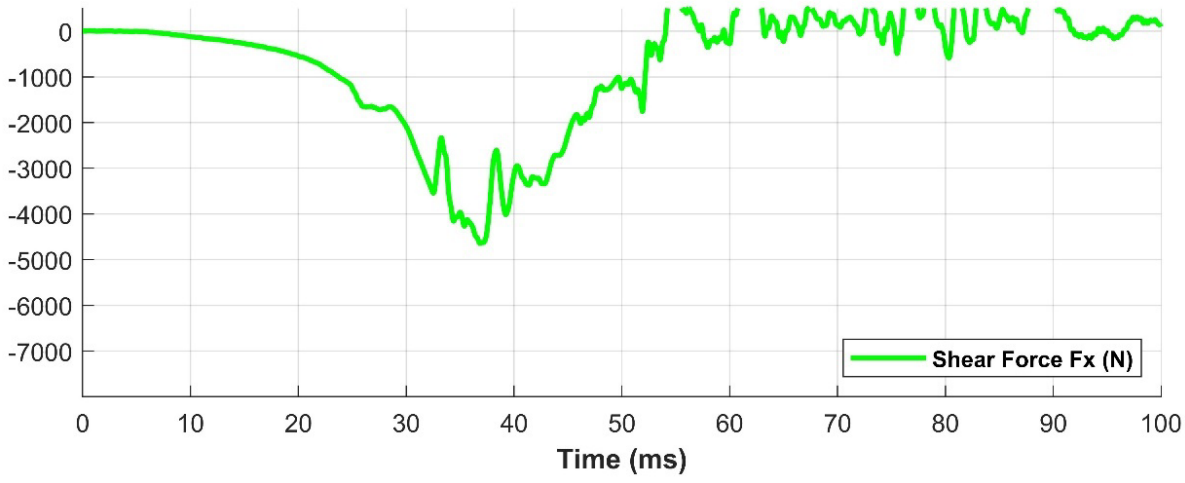
Shear Force Fx (N)
0
-1000
-2000
-3000
-4000
-5000
-6000
-7000
0
10
20
30
40
50
60
70
80
90
100
Time (ms)

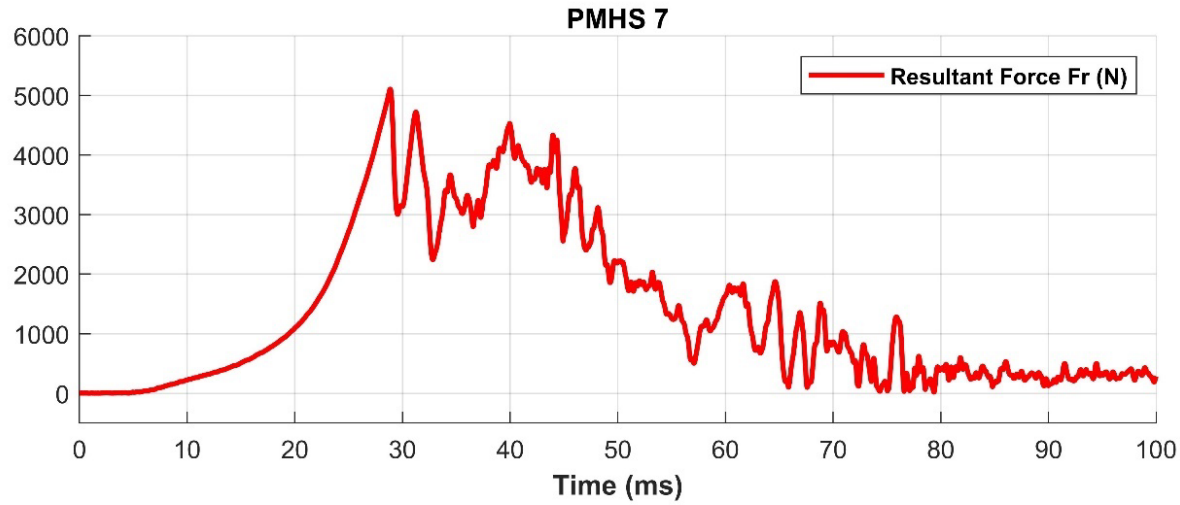
PMHS 7
Resultant Force Fr (N)
6000
5000
4000
3000
2000
1000
0
0
10
20
30
40
50
60
70
80
90
100
Time (ms)

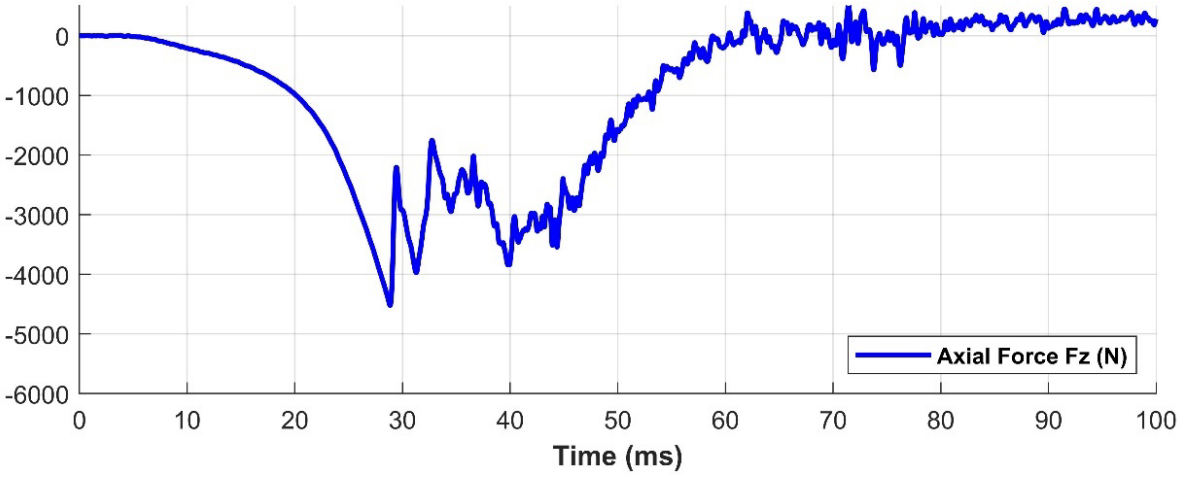
Axial Force Fz (N)
0
-1000
-2000
-3000
-4000
-5000
-6000
0
10
20
30
40
50
60
70
80
90
100
Time (ms)

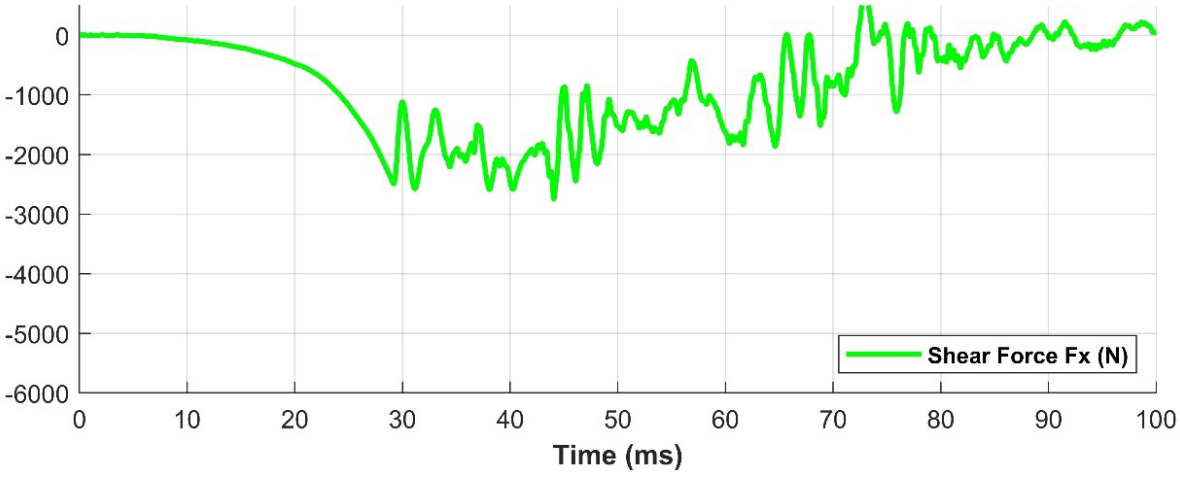
Shear Force Fx (N)
0
-1000
-2000
-3000
-4000
-5000
-6000
0
10
20
30
40
50
60
70
80
90
100
Time (ms)

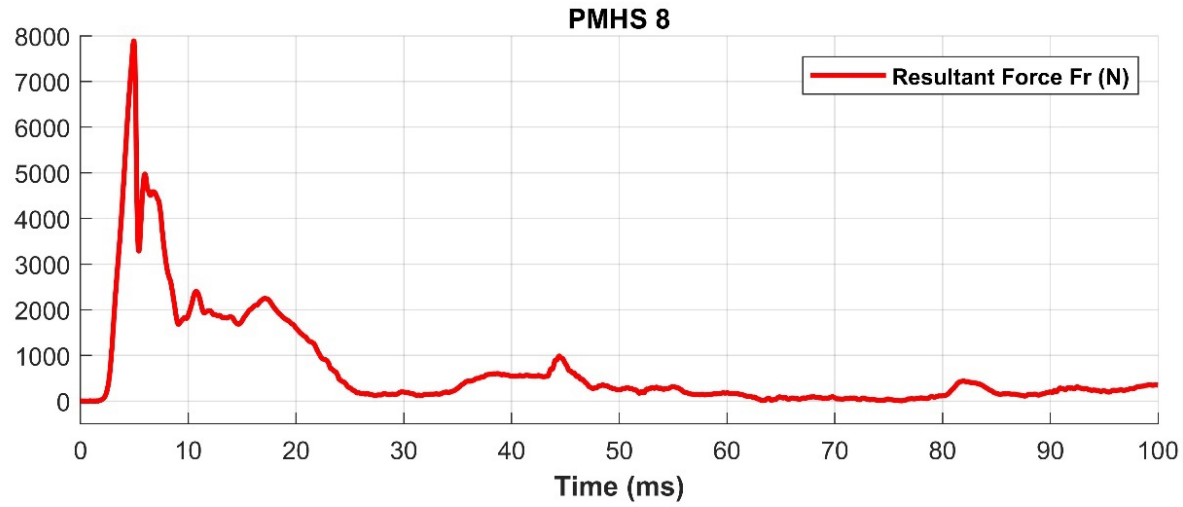
PMHS 8
Resultant Force Fr (N)
8000
7000
6000
5000
4000
3000
2000
1000
0
0
10
20
30
40
50
60
70
80
90
100
Time (ms)

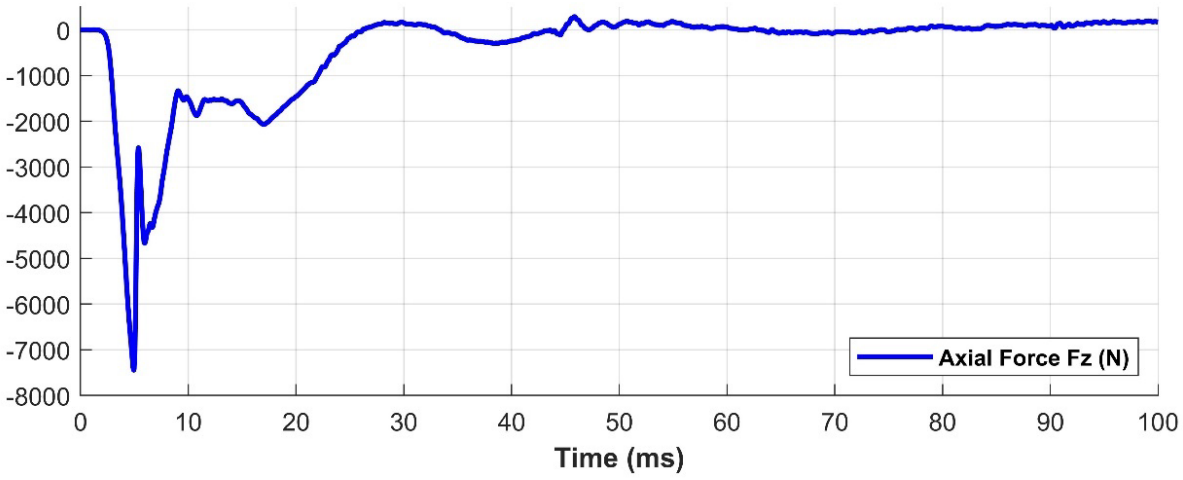
Axial Force Fz (N)
0
-1000
-2000
-3000
-4000
-5000
-6000
-7000
-8000
0
10
20
30
40
50
60
70
80
90
100
Time (ms)

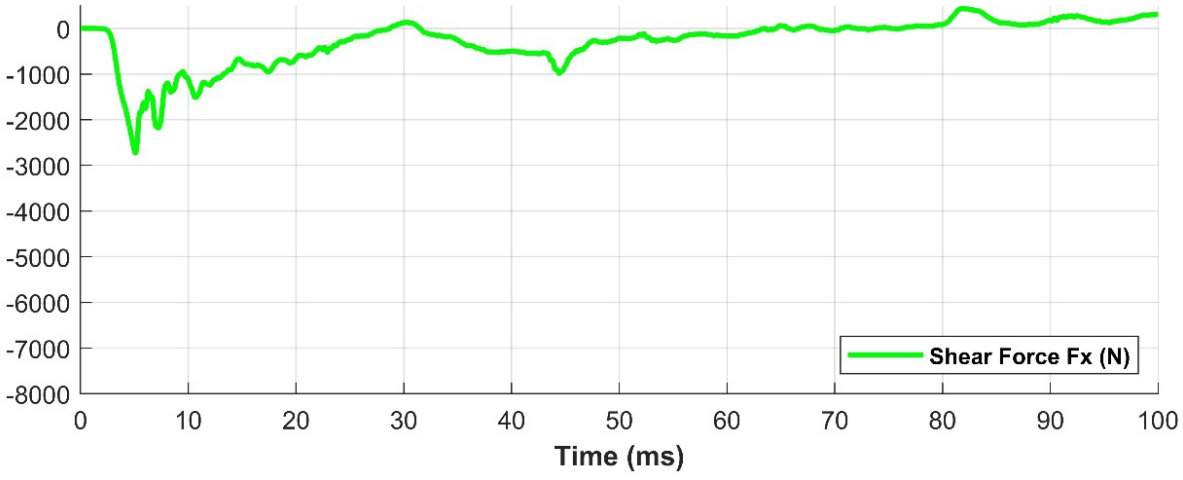
Shear Force Fx (N)
0
-1000
-2000
-3000
-4000
-5000
-6000
-7000
-8000
0
10
20
30
40
50
60
70
80
90
100
Time (ms)

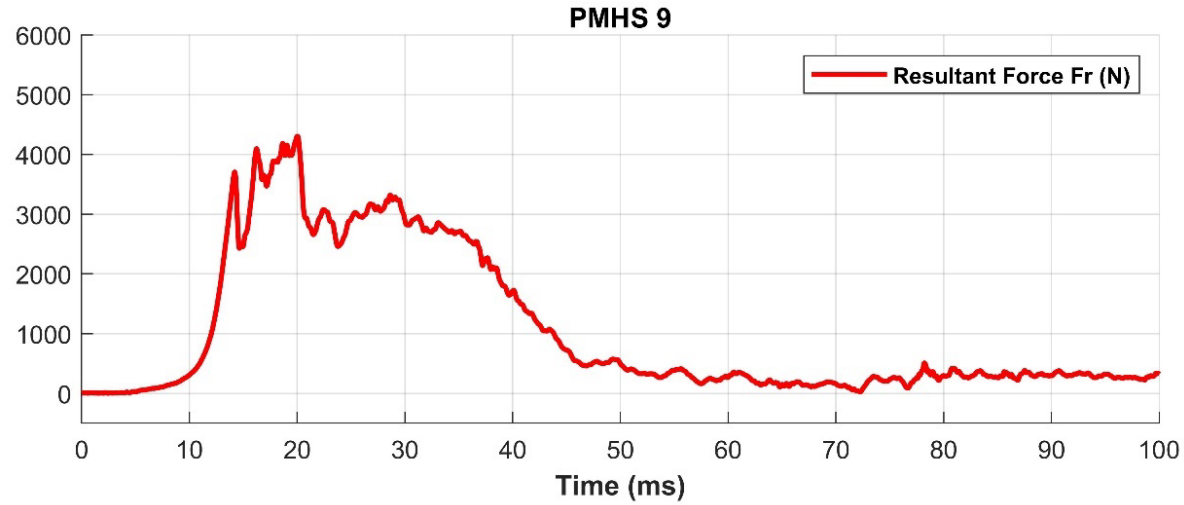
PMHS 9
Resultant Force Fr (N)
6000
5000
4000
3000
2000
1000
0
0 10 20 30 40 50 60 70 80 90 100
Time (ms)

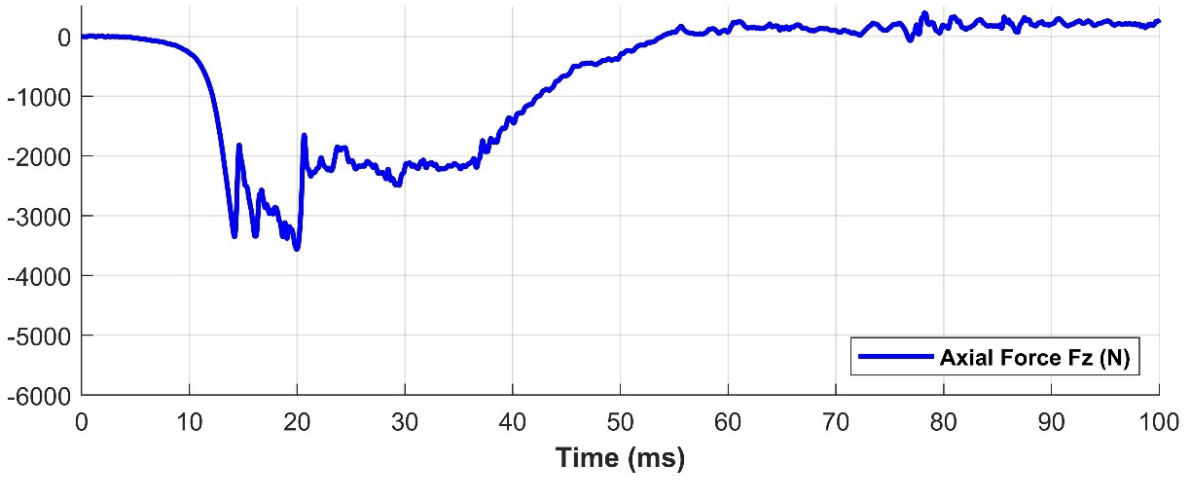
Axial Force Fz (N)
0
-1000
-2000
-3000
-4000
-5000
-6000
0 10 20 30 40 50 60 70 80 90 100
Time (ms)

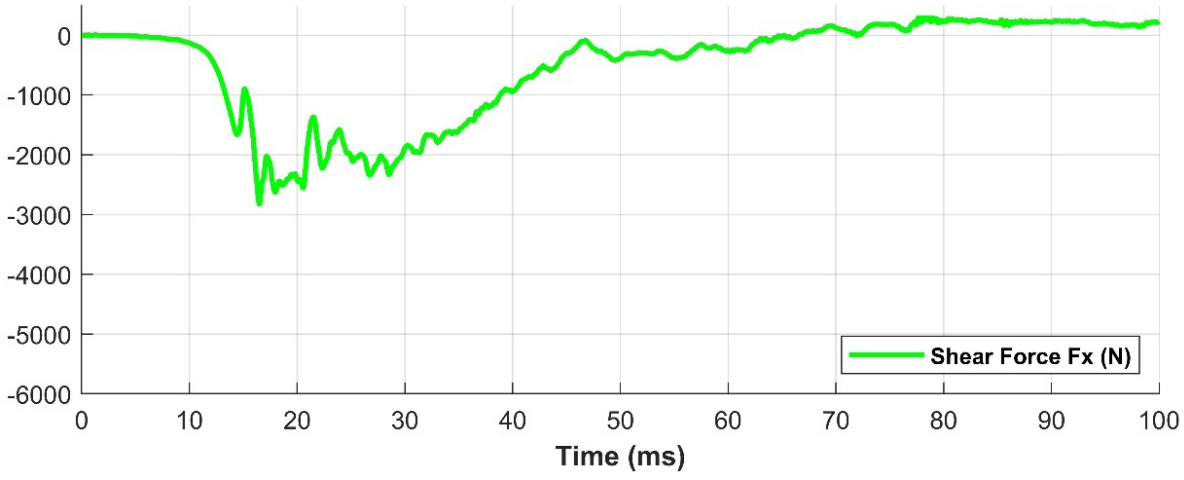
Shear Force Fx (N)
0
-1000
-2000
-3000
-4000
-5000
-6000
0 10 20 30 40 50 60 70 80 90 100
Time (ms)

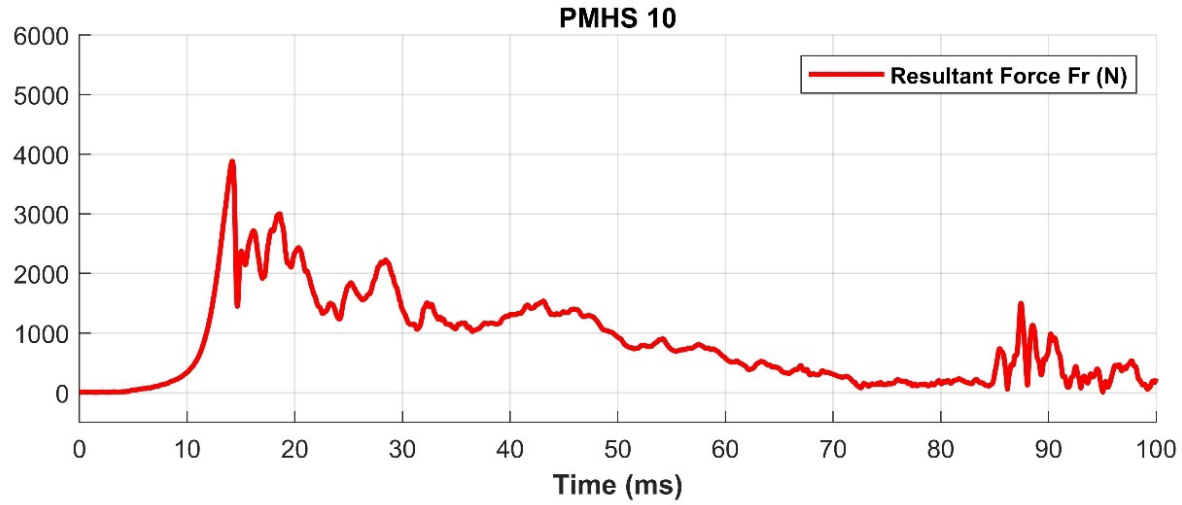
PMHS 10
Resultant Force Fr (N)
6000
5000
4000
3000
2000
1000
0
0
10
20
30
40
50
60
70
80
90
100
Time (ms)

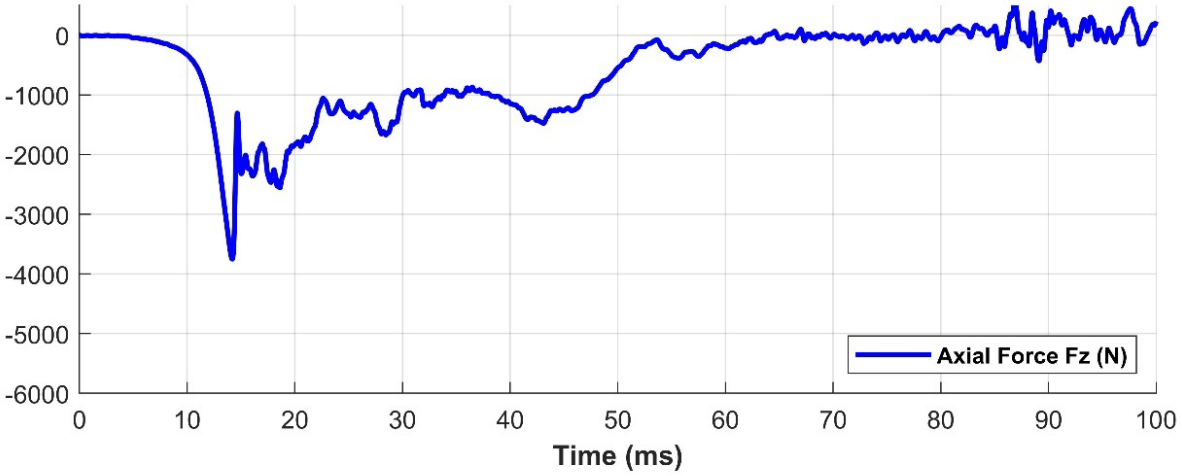
0
-1000
-2000
-3000
-4000
-5000
-6000
Axial Force Fz (N)
0
10
20
30
40
50
60
70
80
90
100
Time (ms)

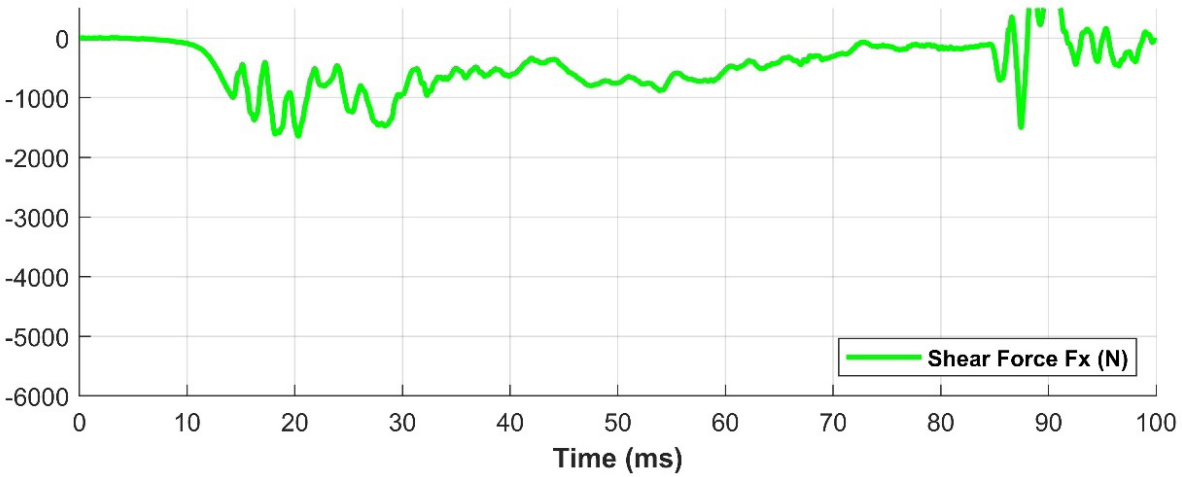
0
-1000
-2000
-3000
-4000
-5000
-6000
Shear Force Fx (N)
0
10
20
30
40
50
60
70
80
90
100
Time (ms)

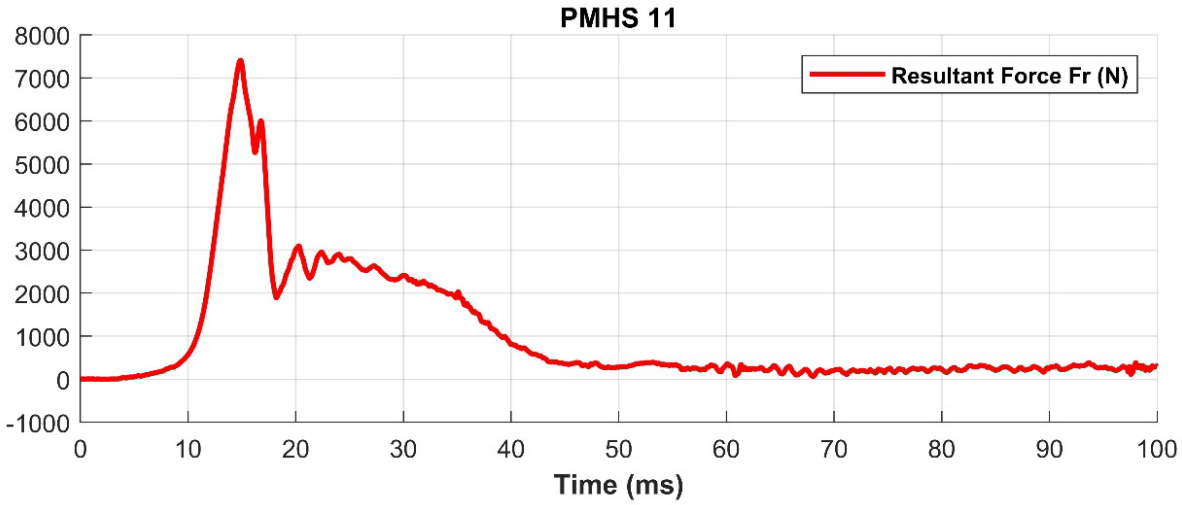
PMHS 11
Resultant Force Fr (N)
8000
7000
6000
5000
4000
3000
2000
1000
0
-1000
0
10
20
30
40
50
60
70
80
90
100
Time (ms)

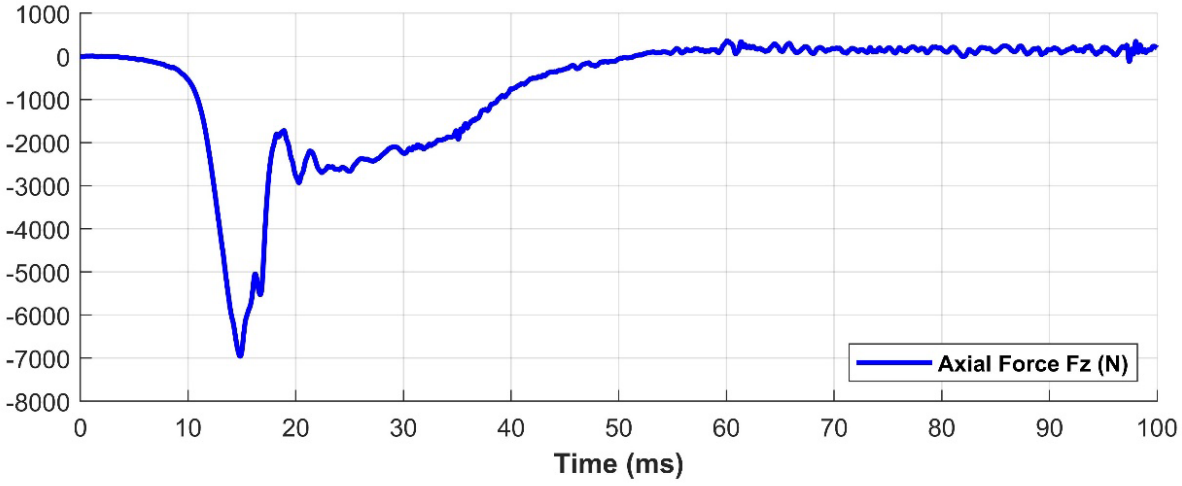
1000
0
-1000
-2000
-3000
-4000
-5000
-6000
-7000
-8000
Axial Force Fz (N)
0
10
20
30
40
50
60
70
80
90
100
Time (ms)

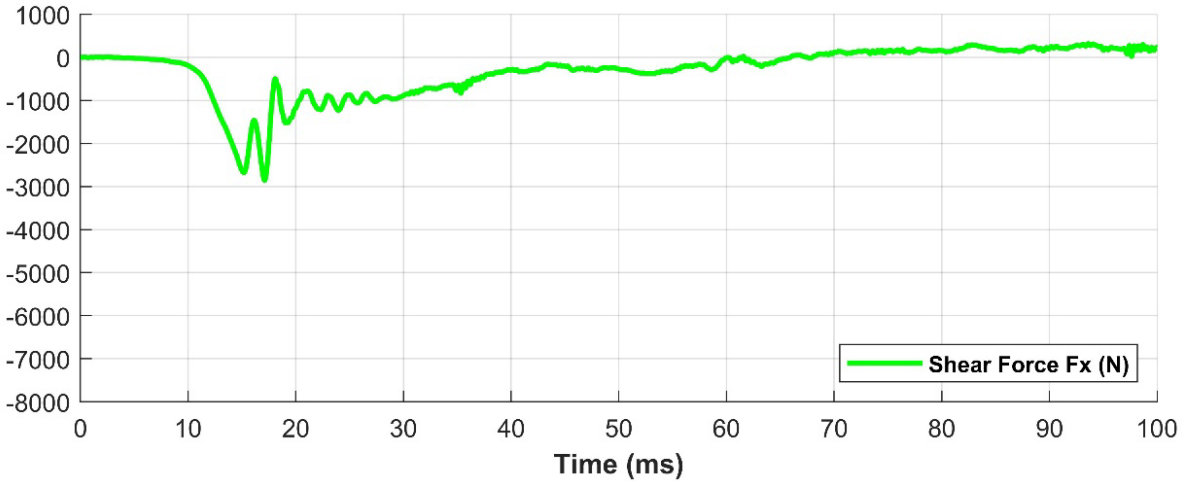
1000
0
-1000
-2000
-3000
-4000
-5000
-6000
-7000
-8000
Shear Force Fx (N)
0
10
20
30
40
50
60
70
80
90
100
Time (ms)

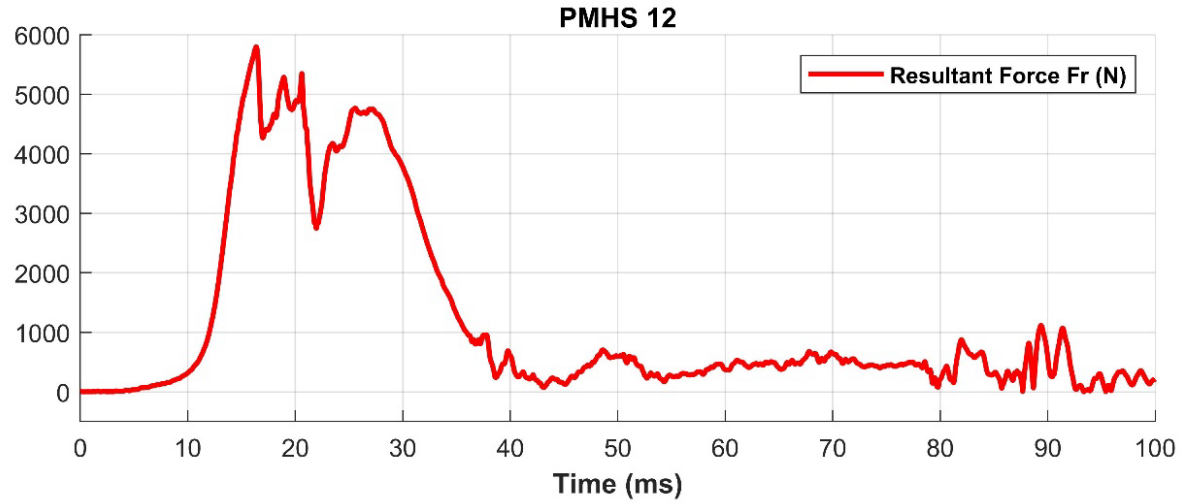
PMHS 12
Resultant Force Fr (N)
6000
5000
4000
3000
2000
1000
0
0
10
20
30
40
50
60
70
80
90
100
Time (ms)

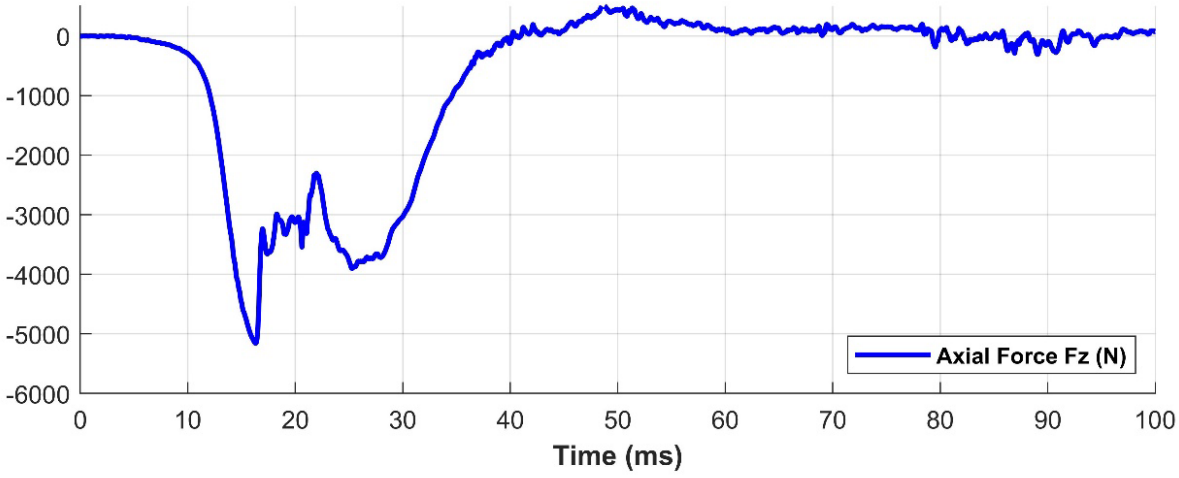
Axial Force Fz (N)
0
-1000
-2000
-3000
-4000
-5000
-6000
0
10
20
30
40
50
60
70
80
90
100
Time (ms)

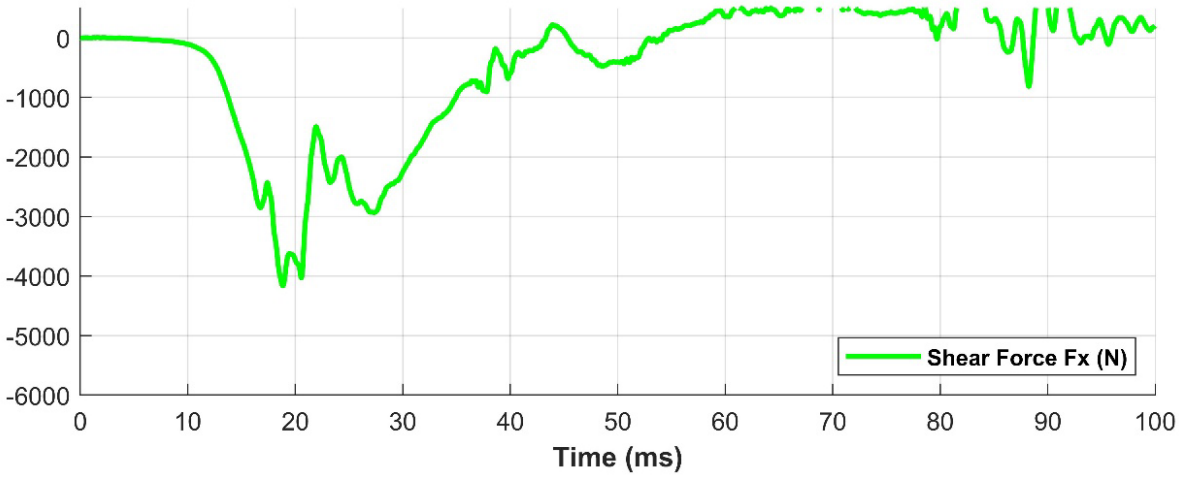
Shear Force Fx (N)
0
-1000
-2000
-3000
-4000
-5000
-6000
0
10
20
30
40
50
60
70
80
90
100
Time (ms)

Appendix E – List of Acronyms

AIS	Abbreviated Injury Scale
ATD	Anthropomorphic Test Device
BSM	Brier score metric
CT	computed tomography
HAIS	Highest Abbreviated Injury Scale
IARC	Injury Assessment Reference Curve
IED	improvised explosive device
PMHS	postmortem human subject
UBB	under-body blast
WIAMan	Warrior Injury Assessment Manikin

Appendix F – Distribution List

ORGANIZATION

DEVCOM Analysis Center
FCDD-DAD-TP/G. Dietrich
FCDD-DAG/N. Eldredge
FCDD-DAG-S/K. Loftis
FCDD-DAG-S/D. Barnes
FCDD-DAG-S/K. Sandora
FCDD- DAG-S/G. Steiger
FCDD- DAG-S/B. Vanamburg
6896 Mauchly St.
Aberdeen Proving Ground, MD 21005-5071

DEVCOM Army Research Laboratory
FCDD-RLD-DCI/Tech Library
2800 Powder Mill Rd.
Adelphi, MD 20783

Defense Technical Information Center
ATTN: DTIC-O
8725 John J. Kingman Rd.
Fort Belvoir, VA 22060-6218

U.S. Army Evaluation Center
Survivability Evaluation Directorate
TEEC-SV/RJ Spink
6617 Aberdeen Blvd., Bldg 2202, 2nd Floor
Aberdeen Proving Ground, MD 21005-5071

DEVCOM Ground Vehicle Systems Center
FCDD-GVR-VMT/D. Weyland
FCDD-GVR-VMT/R. Scherer
6501 E. 11 Mile Rd
Detroit Arsenal, MI 48397-5000

Office of the Director, Operational Test and Evaluation
OSD DOT&E
LFT&E/S. Bartyczak
1700 Defense Pentagon 1D548
Washington, DC 20301

Medical College of Wisconsin
N. Yoganandan
J. Moore
J. R. Humm
F. A. Pintar
J. Baisden
8701 W. Watertown Plank Rd.
Milwaukee, WI 53226